MEMBRANE TOPOLOGY OF BCL-X_L

A Fluorescence-based Method for Studying the Membrane Topology of the Anti-apoptotic protein Bcl-X_L

By

Helen M. Atkinson, B.Sc.

A Thesis

Submitted to the School of Graduate Studies

in Partial Fulfillment of the Requirements

for the Degree

Master of Science

McMaster University

MASTER OF SCIENCE (2001)
(Biochemistry)

McMaster University
Hamilton, Ontario

TITLE:	A fluorescence-based method for studying the membrane topology of the anti-apoptotic protein Bcl-X_L.
AUTHOR:	Helen M. Atkinson, B.Sc. (University of Waterloo)
SUPERVISOR:	Dr. David W. Andrews
NUMBER OF PAGES:	xi, 77

Abstract

Bcl-X_L is a membrane-associated protein that inhibits programmed cell death (apoptosis) in mammalian cells. Very little is known about the membrane topology of Bcl-X_L or how its association with membranes contributes to its function. It was the aim of this thesis to use fluorescence spectroscopy to investigate the location of a specific amino acid of Bcl-X_L relative to the membrane.

Bcl-X_L purified from *E. coli* could bind both to large unilamellar vesicles and endoplasmic reticulum (ER) microsomes isolated from canine pancreas. A cysteine residue at position 151 in Bcl-X_L could be covalently labelled with the environmentally sensitive fluorescent molecule NBD. Emission intensity measurements in the presence and absence of membranes, combined with aqueous and lipophilic quenching experiments, indicate that Cys151 is inserted into the interior of the membrane bilayer when Bcl-X_L is bound to membranes. The methods outlined in this thesis form the basis for an experimental system that can be used to determine the membrane topology of Bcl-X_L under a variety of conditions.

Acknowledgements

I would like to thank my supervisor, Dr. David W. Andrews, for his guidance throughout my graduate studies. I would also like to thank my committee members, Dr. Brian Leber and Dr. Eric Brown, for all of their helpful contributions.

All of the people who have passed through the Andrews Lab have made my graduate career an enjoyable experience. I would especially like to thank Mina Falcone for her invaluable and enduring friendship. I also want to acknowledge Aline Fiebig, Peter Kim, Kyle Legate and Cliff Dominy for many helpful discussions, both scientific and personal. Also thanks to Iain Mainprize for help with RasMol, and library resources.

Dr. Arthur Johnson, Texas A&M University, and Alejandro Heuck let me into their lab for two weeks and taught me the basics of doing fluorescence experiments, and I am very grateful for their useful suggestions throughout the completion of this degree.

I would like to acknowledge the financial support of Dr. Andrews, and the NSERC Scholarship Program.

Finally, and most importantly, thanks go to my parents and to Jerry Han for all their love and support over the years.

Table of Contents

List of Abbreviations

7-NO-PC	1-palmitoyl-2-stearoyl-(7-doxyl)-phosphatidylcholine
BH	Bcl-2 homology
BSA	bovine serum albumin
CBD	chitin binding domain
CHAPS	3-[(3-cholamidopropyl)dimethylammonio]-1-propane sulfonate
cmc	critical micelle concentration
CRM	canine rough microsome
DOPC	dioleoylphosphatidylcholine
DOPG	dioleoylphosphatidylglycerol
DTT	dithiothreitol
EDTA	ethylenediaminetetraacetic acid
eq	equivalents of CRMs (1 eq/μL of CRMs = 50 A_{280} units/mL)
EKRM	CRM column-washed and extracted with 0.5M KOAc and 50mM EDTA
ER	endoplasmic reticulum
Hepes	*N*-2-hydroxyethylpiperazine-*N'*-2-ethanesulfonic acid
HRP	horseradish peroxidase
IANBD	*N,N'*-dimethyl-*N*-(iodoacetyl)-*N'*-(7-nitrobenz-2-oxa-1,3-diazolyl)ethylenediamine

IPTG	isopropyl-β-D-thiogalactoside
KOAc	potassium acetate
LB	Luria Broth
LUV	large unilamellar vesicle
PCR	polymerase chain reaction
PIN	protease inhibitors
SDS-PAGE	sodium dodecylsulphate polyacrylamide gel electrophoresis
Srβ	beta subunit of SRP receptor
SRP	signal recognition particle
Tris	Tris(hydroxymethyl)aminomethane

List of Figures

Chapter 1: Introduction

1.1 Introduction to Apoptosis

Apoptosis is a programmed form of cell death that plays an important role in the development and maintenance of eukaryotic tissues. It has been described in such diverse situations as cell turnover in healthy tissues, embryonic development, atrophy, and cell death caused by radiation or various cytotoxic agents (Wyllie *et al.*, 1980). A number of diseases have been associated with defects in the regulation of apoptosis. Apoptosis which occurs at inappropriate times can contribute to degenerative diseases such as Alzheimer's or Parkinson's disease. Infection with HIV leads to increased death of T cells by apoptosis, possibly contributing to AIDS. In contrast, an inability to undergo apoptosis is a contributing factor in viral infections, autoimmune disease, and cancer (Thompson, 1995). A cell undergoing apoptosis exhibits a number of characteristic morphological and biochemical hallmarks that are distinct from the changes seen in other forms of cell death, such as necrosis (Wyllie *et al.*, 1980). Examples of these include chromatin condensation, cell blebbing, cell shrinkage, cleavage of specific cellular proteins, and the formation of apoptotic bodies.

The executioners of apoptosis are the caspases, a family of cysteine proteases that cleave after specific aspartic acid residues (reviewed in Thornberry and Lazebnik, 1998). Caspases exist as proenzymes in the cell until they are proteolytically activated following

a proapoptotic signal. The initiator caspases (caspase-8, -9) initiate cleavage of the effector caspases (caspase-3, -6, -7) producing a caspase cascade which targets numerous cellular factors. Caspase targets are involved in such diverse activities as DNA repair, DNA replication, and inhibiting DNA fragmentation and chromatin condensation, as well as cytoskeleton regulation and adhesion.

While the events that occur during apoptosis have been extensively studied, of more interest is the manner in which the cell regulates this particular form of cell death.

1.2 *Caenorhabditis elegans* model of apoptosis

Some of the earliest studies of apoptosis regulation evolved through work with the nematode *Caenorhabditis elegans*. *C. elegans* is useful as a model organism for genetic studies of programmed cell death because of its small size, invariant anatomy, and the fact that the majority of programmed somatic cell deaths occur by the same mechanism (Ellis and Horvitz, 1986). Generation of mutant worms unable to undergo apoptosis led to the isolation of a number of genes responsible for this process, the three most important being ced-3, ced-4 and ced-9. Ced-3 and ced-4 are required for cell death, whereas ced-9 has a cytoprotective function (Ellis and Horvitz, 1986; Hengartner *et al.*, 1992). These three molecules have been shown to interact, with ced-4 providing the link between the death effector ced-3 and the protector ced-9 (Chinnaiyan *et al.*, 1997).

Based on the above-mentioned studies, and others, a model for the regulation of apoptosis in *C. elegans* has been proposed (reviewed in Reed, 1997; Horvitz, 1999). In

this model, ced-4 acts as a molecular switch by binding to ced-3 in the cytosol, activating it and initiating apoptosis (Figure 1A). However, if ced-9 is present it binds to the ced-3/ced-4 complex, sequestering it on the membrane surface and preventing the activation of ced-3 (Figure 1B). A death promoting protein such as egl-1 (Conradt and Horvitz, 1998) can associate with ced-9, releasing the ced-4/ced-3 complex and allowing apoptosis to proceed (Figure 1C).

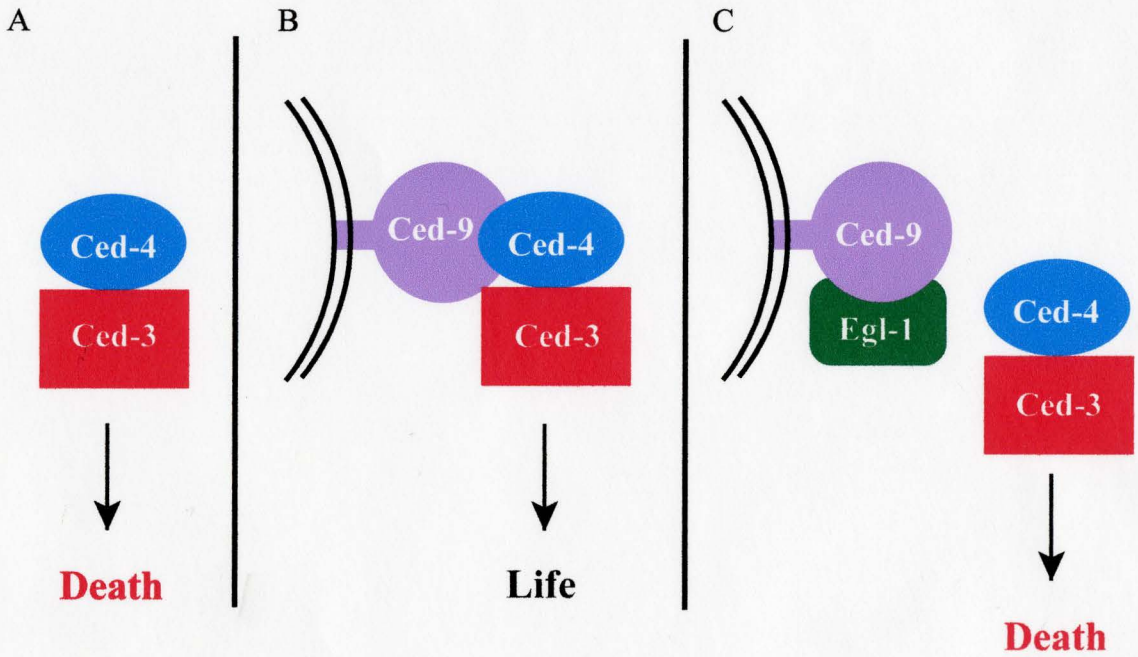

Figure 1: **Model of apoptosis in the nematode *Caenorhabditis elegans*** (adapted from Reed, 1997).

Mammalian homologues to each of these *C. elegans* proteins have been discovered. Ced-3 is a member of the caspase family. The mammalian ced-4 homologue, Apaf-1 is required for caspase activation (Zou *et al.*, 1997), and can form a ternary complex with caspase-9 and Bcl-X_L (Pan *et al.*, 1998). Bcl-X_L is a ced-9 homologue and belongs to the Bcl-2 family of apoptosis-regulators, a subset of which shows similarity to egl-1.

1.3 The Bcl-2 protein family

The Bcl-2 protein is the prototype of a large family of proteins that have been identified as regulators of apoptosis in mammals. Bcl-2, was first isolated as part of a common translocation seen in B cell lymphomas. The t(14:18) translocation places the gene for Bcl-2 behind the IgG promoter, where its expression is upregulated, causing an inhibition of apoptosis (Cleary *et al.*, 1986). Since that time, a number of Bcl-2-related proteins have been discovered.

The Bcl-2 family can be divided into two main groups; those that inhibit apoptosis, and those that promote apoptosis (Figure 2). Sequence alignment of the Bcl-2 family proteins have identified four conserved Bcl-2 homology regions (BH1, BH2, BH3, and BH4), that play a role both in apoptosis regulation and in protein-protein interactions within the family (reviewed in White, 1996; Rao and White, 1997; Korsmeyer, 1999). Most of the anti-apoptotic family members contain at least BH1 and BH2. The pro-apoptotic proteins are subdivided into two groups: those that have BH1-3, and those that show homology only in the BH3 domain. Mutations in the BH1 and BH2 domains of

Bcl-2 have been shown to abrogate both its ability to bind to Bax and its death-repressing activity (Yin *et al.*, 1994). In contrast to the anti-apoptotic proteins, death promoters such as Bax appear to require the BH3 domain alone for activity and interaction with other family members (Zha *et al.*, 1996). The existence of the "BH3 only" proteins supports the theory that BH3 is the minimal "death domain" required for initiating apoptosis.

Bcl-2, and many of its homologues, contain a C-terminal membrane insertion sequence capable of targeting Bcl-2 post-translationally to membranes (Janiak *et al.*, 1994a). This sequence consists of a group of hydrophobic residues at the C-terminal tail of the protein, long enough to span a membrane, and flanked on either side by positively charged residues. The insertion sequence mediates the integration of the protein into the membrane in a Signal Recognition Particle-independent manner. Bcl-2 has been shown to bind to the endoplasmic reticulum (ER) and the outer mitochondrial membrane, with the bulk of the protein facing the cytosol (Janiak *et al.*, 1994a). Evidence has been gathered indicating that this membrane binding is crucial for function. Deletion of the insertion sequence, creating a cytosolic form of Bcl-2, seriously impairs its ability to protect against apoptosis from a number of stimuli (Zhu *et al.*, 1996; Nguyen *et al.*, 1994).

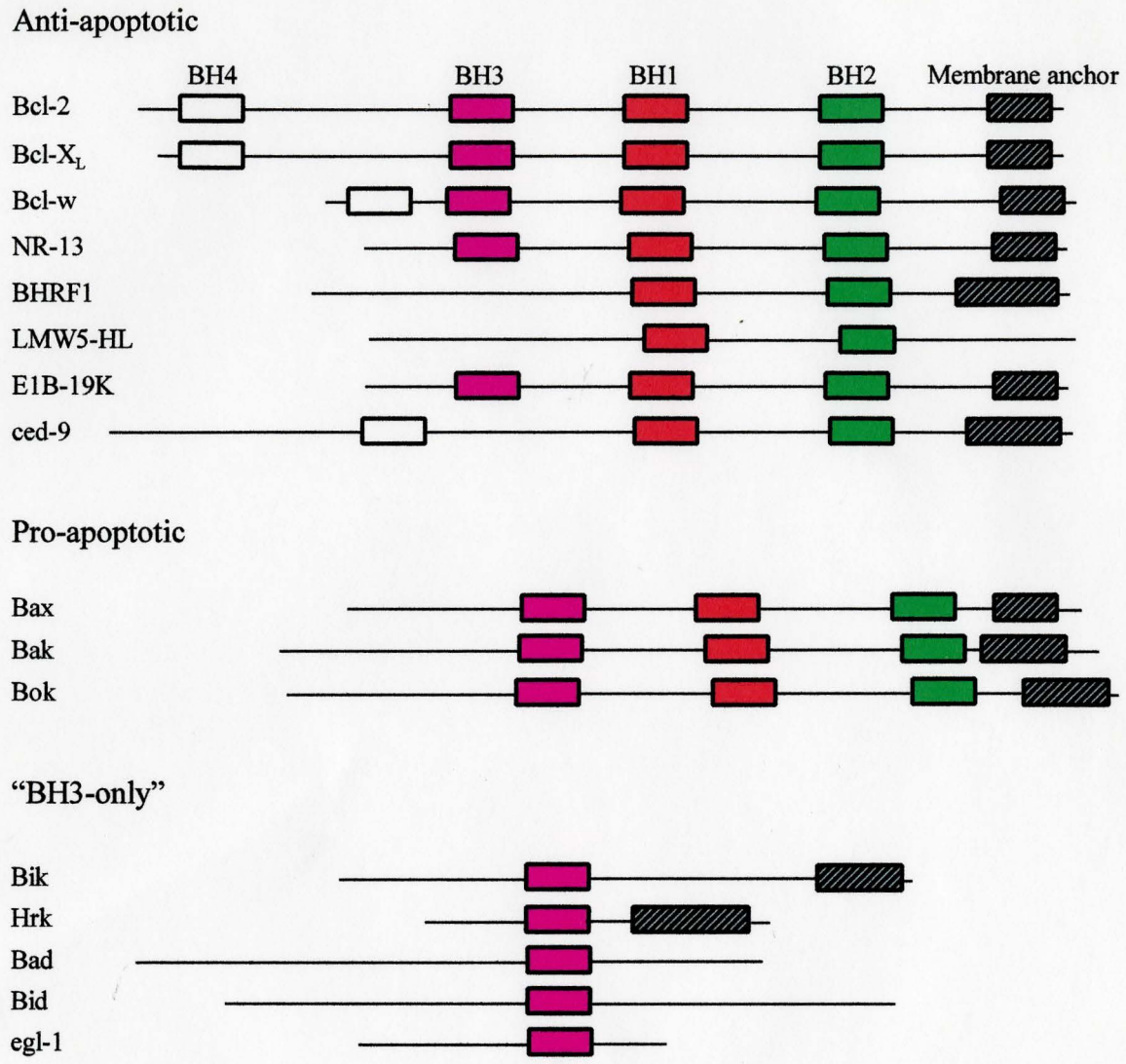

Figure 2: **The Bcl-2 protein family.**
Some of the Bcl-2 family members are shown. The conserved BH domains in each family member are indicated, as well as the C-terminal membrane anchor sequence. NR-13 is a chicken protein, and ced-9 and egl-1 are from *C. elegans*. BHRF1, LMW5-HL, and E1B-19K are viral proteins. The rest are mammalian. (Adapted from Adams and Cory, 1998; Gross *et al.*, 1999).

1.4 Introduction to Bcl-X_L

The *bcl-x* gene was first identified in chicken lymphoid cells using a low stringency screen of a cDNA library with a murine *bcl-2* probe. Two splice variants of the gene, bcl-X_L and bcl-X_S were subsequently identified in humans. Bcl-X_L is an anti-apoptotic protein which has significant sequence homology with Bcl-2 (Boise *et al.*, 1993).

Bcl-X_L has been reported to bind to the outer mitochondrial membrane (González-Garcia *et al.*, 1994). It has also been shown to interact with proteins found on the ER (Ng and Shore, 1998). Other studies have found that it exists in both the cytosolic and membrane-bound fractions in non-apoptotic cells, but shifts entirely to the membrane-bound fraction upon induction of apoptosis (Hsu and Youle, 1997; Hsu *et al.*, 1997). The C-terminal insertion sequence appears to be necessary for the full anti-apoptotic activity of Bcl-X_L. Its deletion prevents Bcl-X_L from targeting intracellular membranes and partially inhibits the ability of Bcl-X_L to prevent apoptosis (Wolter *et al.*, 1997).

Bcl-X_L is constitutively expressed in adult human brain tissue, suggesting it has a role in the long-term maintenance of neural tissue following development (Boise *et al.*, 1993). In mice Bcl-X_L is highly expressed in tissues during embryonic and postnatal development. Bcl-X_L was found in considerably higher levels than Bcl-2 in adult brain, thymus, and kidney, whereas Bcl-2 was more abundant in lymph nodes (Gonzalez-Garcia *et al.*, 1994). Bcl-$x^{-/-}$ mice displayed an embryonic lethal phenotype, with extensive cell death throughout the brain and spinal cord (Motoyama *et al.*, 1995).

1.5 Structure of Bcl-X_L

Bcl-X_L was the first of the Bcl-2 family proteins to have its crystal and solution structures published (Muchmore *et al.*, 1996), although the recombinant protein used in the structural analysis lacked the transmembrane region needed for membrane binding. In solution Bcl-X_L forms a compact bundle of seven α-helices (Figure 3A). Two central α-helices, α5 and α6, are approximately 30 Å in length and predominantly hydrophobic. They are arranged in an anti-parallel manner and are surrounded on one side by α3 and α4, and on the other by α1, α2 and α7. The BH1, 2 and 3 domains are in close proximity and create an elongated hydrophobic region. A Bak peptide encompassing the BH3 region was found to bind in this region of Bcl-X_L (Sattler *et al.*, 1997).

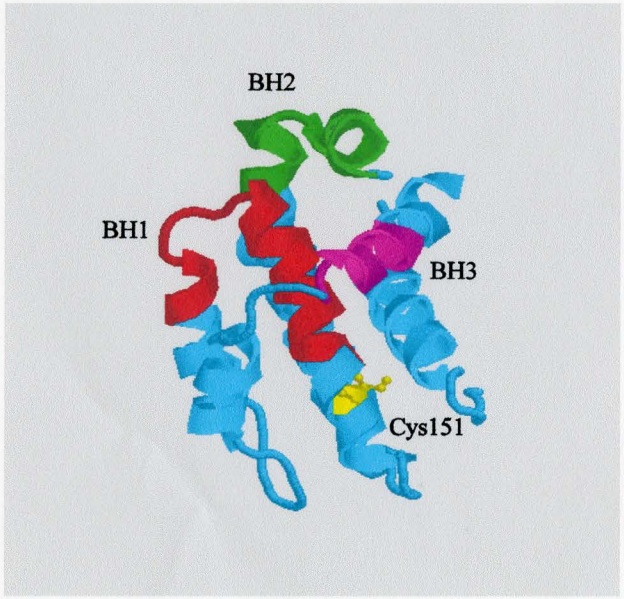

Figure 3A: **Structure of Bcl-X_L.**
Ribbon depiction of the solution structure of Bcl-X_L. BH1, 2 and 3 domains are coloured red, green and magenta respectively. Cys151 is in yellow and the position of its sidechain is shown (adapted from Muchmore *et al.*, 1996).

The structure of Bcl-X_L also indicated a marked similarity to certain pore-forming proteins, such as the membrane insertion domain of diphtheria toxin (Figure 3B). It was therefore suggested that the Bcl-2 protein family may carry out their function by forming pores in the membrane, either alone or in combination with other family members.

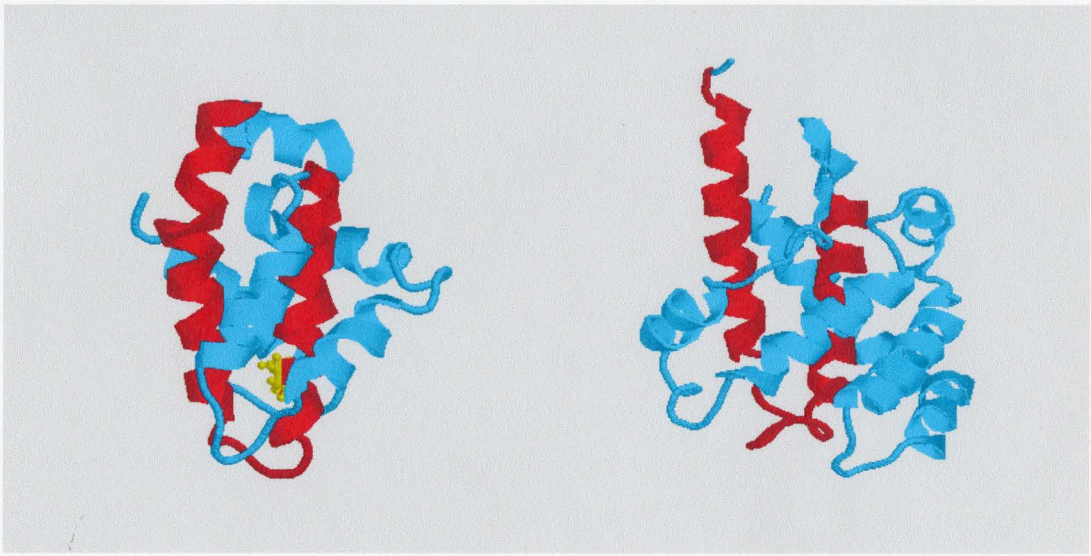

Bcl-X_L Diphtheria toxin

Figure 3B: Comparison of Bcl-X_L and diphtheria toxin.
The structures of Bcl-X_L and the transmembrane domain of diphtheria toxin are shown. The two central α-helices of each protein (α5 and α6 in Bcl-X_L, TH8 and TH9 of diphtheria toxin) are coloured red. The position of Cys151 of Bcl-X_L (in yellow) is indicated (adapted from Muchmore *et al.*, 1996; Bennett *et al.*, 1994).

Active diphtheria toxin consists of two disulfide-linked fragments, A and B. Fragment A is the catalytic domain, inhibiting protein synthesis and thereby killing the cell. In order to exert its effect, Fragment A must first enter the cytoplasm, a process carried out by Fragment B. Fragment B has two domains, a receptor-binding domain and a transmembrane domain. The receptor-binding domain is responsible for recognizing a receptor at the cell surface, causing the toxin to be internalized by endocytosis. The acidic conditions within the endosome are believed to cause partial unfolding of the toxin, exposing hydrophobic regions which insert into the bilayer (Jiang *et al.*, 1991). It is believed that the transmembrane domain forms a pore which allows translocation of Fragment A across the membrane, although the exact nature of the translocation event remains uncertain. Crystalization of the transmembrane domain (Choe *et al.*, 1992; Bennett *et al.*, 1994) revealed that it was composed of nine α-helices (TH1-9) with the central helices, TH8 and TH9, being extremely hydrophobic. TH6 and TH7 are also fairly hydrophobic, while TH1-3 are hydrophilic. The loop between TH8 and TH9, is acidic, containing Asp and Glu residues. It was suggested based on this structure that in the acidic endosomal conditions the loop residues would become protonated, making them more membrane-soluble and allowing TH8 and TH9 to insert into the membrane. This theory is supported by experiments in which two acidic amino acids in the loop region connecting TH8 and TH9 were mutated to lysine (Ren *et al.*, 1999). The mutants showed a marked reduction in transmembrane insertion and pore formation, although these functions were not entirely inhibited indicating that there are other factors beside helix tip neutralization involved in membrane insertion.

Based on the comparison of Bcl-X_L to diphtheria toxin, ion conductance experiments were carried out on some Bcl-2 family members at acidic pH to determine if they could form pores. Bcl-X_L, Bcl-2 and Bax induced bulk ion efflux from synthetic lipid vesicles at pH 4, but this efflux was inhibited at physiological pH (Schendel *et al.*, 1997; Schlesinger *et al.*, 1997; Minn *et al.*, 1997). It is uncertain how relevant these studies may be since they were done with recombinant proteins that lack the C-terminal transmembrane sequence. In addition, unlike diphtheria toxin, it is unlikely that the Bcl-2 family members would encounter the acidic conditions that were necessary for bulk pore-formation in these experiments *in vivo*. Single-channel recordings, a more sensitive technique, have measured channel activity at physiological pH for both the truncated molecules and full-length Bcl-X_L (Minn *et al.*, 1997; Lam *et al.*, 1998). How channel activity may relate to the anti-apoptotic function of Bcl-X_L is not known.

1.6 Objective of Thesis

The crystal structure of soluble Bcl-X_L has raised interesting speculation about its membrane topology and function. Based on the structural comparison with diphtheria toxin the hypothesis is that the two central hydrophobic alpha helices, $\alpha 5$ and $\alpha 6$, insert into the lipid bilayer. However the membrane topology of this region of Bcl-X_L has never been experimentally determined.

The objectives of this study were to target recombinant Bcl-X_L to intracellular membranes under near to physiological conditions, and to develop a fluorescence-based appoach to studying the membrane topology of Bcl-X_L. In human Bcl-X_L there is a single

cysteine residue occurring at position 151 which is near the C-terminal end of the α5 helix. By placing a fluorescent dye on this residue and using a variety of complementary fluorescence techniques to investigate the local environment of this cysteine when Bcl-X_L is bound to membranes, I have determined that Cys151 is inserted into the lipid bilayer.

Chapter 2: Materials and Methods

2.1 General Materials

General chemical reagents were obtained from either Gibco-BRL, Sigma Chemicals, BioShop Inc. or Fisher Scientific. Restriction enzymes were obtained from MBI Fermentas Inc. or New England Biolabs. IMPACT™ cloning vectors, sequencing primers, and chitin beads were purchased from New England Biolabs. 3-[(3-cholamidopropyl)dimethylammonio]-1-propane sulfonate (CHAPS) was purchased from Boehringer Mannheim and Sigma. SP6 polymerase was purchased from Epicenter Technologies. [^{35}S]-methionine was from Perkin Elmer Life Sciences. Hydroxylamine was purchased from Sigma. *N*,*N*'-dimethyl-*N*-(iodoacetyl)-*N*'-(7-nitrobenz-2-oxa-1,3-diazol-4-yl)ethylenediamine (IANBD) was purchased from Molecular Probes. All lipids were purchased from Avanti Polar Lipids.

Primary polyclonal antibodies to Bcl-X_L were generated against full-length human Bcl-X_L. Sheep α-Bcl-X_L (Exalpha Biologicals) was used at a dilution of 1:5000 in western blots. Rabbit α-Bcl-X_L (made by Domina Falcone and Aline Fiebig, McMaster University) was used at a dilution of 1:20000, unless otherwise noted. Calreticulin antibody and cytochrome c antibody were purchased from Exalpha Biologicals, and hsp60 antibody was a kind gift from Dr. R. Gupta, McMaster University. Calreticulin antibody was used at a dilution of 1:5000, cytochrome c antibody was used at a 1:2500

dilution, and hsp60 antibody was used at a 1:10000 dilution. HRP-linked secondary antibodies (donkey α-rabbit and donkey α-sheep) were obtained from Jackson Laboratories and were used at a dilution of 1:10000.

Rabbit reticulocyte lysate was prepared by Domina Falcone, McMaster University as previously described (Jackson and Hunt, 1983). Cell free transcription-linked translation reactions were performed as published (Gurevich *et al.*, 1991; Janiak *et al.*, 1994b).

2.1.1 Plasmids

Plasmids used for *in vitro* transcription-linked translation reactions contained the cDNAs of interest under the control of an SP6 promoter, in the vector pSPUTK (Falcone and Andrews, 1991). Details have been published for the plasmids containing pOCTgPA (p495) (Janiak *et al.*, 1994b), and preprolactin (p39) (Falcone and Andrews, 1991). The plasmid containing cytochrome b5 (p10) was a gift from Dr. D. Meyer, University of California (Janiak *et al.*, 1994b). The vector containing a clone for a chimeric Srβ (Young *et al.*, 1995) was engineered to contain an additional glycosylation site at the 5' end of the protein (designated p742) (done by Kyle Legate, McMaster University).

pCYB3-Bcl-X_L (p1132): pCYB3-Bcl-X_L was constructed by Bomina Yu, McMaster University, for overexpression and purification of Bcl-X_L from *E. coli*. A cDNA encoding human Bcl-X_L (obtained from Dr. G. Nuñez, University of Michigan Medical School) was amplified by Polymerase Chain Reaction (PCR) using primers with the

following sequences:

5'-CTGCAGAACCAGTGTGCTGGATCATGAGCCAAAGCAACCGGGAGCTG-3' (The underlined sequence indicates a BspHI site); and

5'-CAGTCCGCTCTTCCGCATTTCCGACTGAAGAGTGAGC-3' (the underlined sequence indicates a SapI site). The second primer removes the stop codon from the Bcl-X_L sequence. The PCR fragment was digested by BspHI and SapI and inserted into pCYB3 (New England Biolabs) using the NcoI and SapI sites in the multiple cloning region (BspHI and NcoI produce complementary ends). This places the Bcl-X_L coding sequence in frame with the intein-CBD coding sequence in pCYB3 and produces a fusion protein with no additional amino acids between the C-terminus of Bcl-X_L and the N-terminus of the intein.

pCYB3-Bcl-C151S (p1413): For overexpression of Bcl-C151S, a point mutation changing Cys151 of Bcl-X_L to Ser was introduced into pCYB3-Bcl-X_L by the method of Hughes and Andrews, 1996. PCR of the entire pCYB3-Bcl-X_L plasmid was performed using the following overlapping primers:

5'-AAGACGTCCCCGCCGAAGGAGAAAAA-3' and

5'-AAGACGTCACTGT***C***CGTGGAAAGCGTAGACAA-3'. The underlined sequences are AatII sites. The bolded nucleotide in the second primer is the site of the mutation, which changes the codon TGC, encoding Cysteine, to TCC which codes for Serine. The PCR product was digested with AatII and then ligated. This intermediate was then redigested with AatII, the ends were blunted using Klenow fragment, and the product was

religated, producing pCYB3-Bcl-C151S.

Nucleotide sequences of the regions of both of the above plasmids that code for Bcl-X_L were confirmed by sequence analysis (MOBIX, McMaster University).

2.1.2 Commonly used Buffers

Column Buffer:	20mM Tris-Cl pH 7.2, 0.1mM EDTA, 1M NaCl, 20% glycerol, 0.2% (w/v) CHAPS
Cleavage Buffer:	20mM Tris-Cl pH 7.2, 0.1mM EDTA, 0.2M NaCl, 20% glycerol, 0.2% (w/v) CHAPS
PS Elution Buffer:	20mM Tris-Cl pH 7.2, 0.1mM EDTA, 20% glycerol, 0.2% (w/v) CHAPS
G-25 Buffer:	10mM Tris-Cl pH 8.0, 50mM KCl, 1mM $MgCl_2$, 0.015% (w/v) CHAPS, 10% glycerol
Targeting Buffer:	10mM Tris-Cl pH 8.0, 50mM KCl, 1mM $MgCl_2$, 0.015% (w/v) CHAPS, 1mM DTT, 1X PIN (20 μg/mL each of chymostatin, antipain, leupeptin, pepstatin, 40 μg/mL aprotinin)
Buffer R:	10mM Tris-Cl pH 8.0, 50mM KCl, 1mM $MgCl_2$

2.2 General Methods

SDS PAGE electrophoresis was done using 10% Tricine gels (Shagger and von Jagow, 1987). Samples were solubilized in Tricine Loading Buffer (0.1M Tris-Cl, pH 8.9,

2mM EDTA, 10% SDS, 20% glycerol, 0.1% bromophenol blue, 0.25M DTT) prior to electrophoresis. *In vitro* synthesized proteins labelled with [^{35}S]-methionine were visualized by exposure of the dried Tricine gel to Kodak Biomax film. Purified proteins were visualized by western blot. Proteins were transferred onto nitrocellulose using a Hoefer semi-phor transblotter (model #TE77) for 1-1.5 hours at 50 mA per gel. The nitrocellulose, gel, and Whatman 3MM filter paper were soaked in Transfer buffer (30mM Tris, 240mM glycine, 20% methanol) prior to assembly of the apparatus. Following transfer, the nitrocellulose was blocked for a minimum of 30 min. at room temperature in Blocking Buffer (10mM KPO_4 pH 7.4, 140mM NaCl, 0.02% NaN_3, 5g/L powdered milk). Blots were washed for a minimum of 5 min. three times in Wash Buffer (10mM KPO_4 pH 7.4, 140mM NaCl, 0.1% Triton X-100), then incubated in primary antibody diluted in Polyclonal Ab Buffer (10mM KPO_4 pH 7.4, 560mM NaCl, 0.1% Triton X-100, 0.02% SDS, 1% BSA) overnight at 4°C. Following exposure to primary antibody blots were washed twice in Wash Buffer and once in TBS-T (10mM Tris-Cl pH 7.4, 500mM NaCl, 0.2% Tween-20) for a minimum of 5 min. each, and then incubated in secondary antibody (1:10000 dilution) in TBS-T containing 1% BSA. Following incubation blots were washed three times for a minimum of 5 min. each in TBS-T, then developed by the ECL method (NEN Life Sciences Products).

2.3 Overexpression and purification of Bcl-X_L from *E. coli*

For the overexpression of Bcl-X_L-intein-CBD fusion protein, 10 ml of LB medium containing 100 μg/ml ampicillin was inoculated with a single colony of DH5α cells

containing pCYB3-Bcl-X_L and grown overnight at 37°C. This culture was used to inoculate a 1 L culture of LB (containing 100 μg/ml ampicillin) which was also grown overnight at 37°C. The saturated 1 L culture was used to seed a 20-30 L culture of LB containing 50 μg/ml ampicillin, which was grown at 37°C in a fermenter until an OD_{600} of 0.6-0.9 was reached. Isopropyl-β-D-thiogalactoside (IPTG) was added to a final concentration of 1mM and the culture was grown for an additional 3-4 hours at 30°C. Cells were harvested using a continuous flow centrifuge. The cell pellet was resuspended in 250 mL of 1% (w/v) NaCl and then centrifuged in 25-35 ml aliquots at 5000xg for 20 min. The pellets were frozen at -20°C until needed.

Each pellet was resuspended in Column Buffer (100 ml per 16 g of cell pellet) and was lysed using a French Press at a pressure of 16000 psi. The lysate was centrifuged at 18000xg for 30 min., followed by an additional centrifugation at 100000xg for 1 hour. The supernatant was either frozen until needed or loaded immediately onto a chitin column as follows.

40 ml of supernatant was loaded onto a 2 ml chitin column. The column was then washed with 40 ml of Column Buffer, followed by 20 ml of Cleavage Buffer. Cleavage of Bcl-X_L from the intein-CBD fragment was initiated by flushing the column with 6 ml of Cleavage Buffer containing 100 mM hydroxylamine, pH 8.0 for 15 min. The column was incubated in this solution overnight. Following incubation, protein was eluted in 40 ml Cleavage Buffer and was either loaded immediately onto a phenyl Sepharose column or stored at -20°C awaiting further purification.

120 ml of chitin column eluate (usually collected from 3 2-ml chitin columns run

in parallel) was loaded onto a 2 ml phenyl Sepharose column. This column was then washed with 20 ml Cleavage Buffer, followed by a 10 ml linear NaCl gradient from 0.2 M to 0 M NaCl in Cleavage Buffer. The protein was then eluted in PS Elution Buffer and stored at -20°C. All of the above column steps were performed at 4°C. In general, between 25 and 50 μg of purified Bcl-X_L per gram of cell pellet was recovered following the full purification procedure.

2.3.1 Quantification of purified protein

The concentration of purified Bcl-X_L was determined by BCA assay (Pierce) or by measuring the absorbance at 280 nm (both methods gave identical results). The concentration of Bcl-C151S was determined by measuring the absorbance at 280 nm. BSA (Pierce) was used for the concentration standards for the BCA assay. The extinction coefficient of Bcl-X_L at 280 nm was estimated to be 47630 cm^{-1} M^{-1}, and the extinction coefficient of Bcl-C151S was estimated to be 47510 cm^{-1} M^{-1}, based on the number of tryptophans, tyrosines, and cysteines in the protein (Gill and von Hippel, 1989).

2.4 Production of membranes and binding of Bcl-X_L

Canine pancreatic microsomes (CRMs) were prepared by Domina Falcone, McMaster University, and myself according to published procedures (Walter and Blobel, 1983). Amounts of CRMs are expressed as equivalents (eq), where 1 eq/μL = 50 A_{280} units/mL (Walter and Blobel, 1983). EKRMs were prepared by column-washing CRMs and incubating them with 0.5M KOAc and 50mM EDTA, according to published

procedures (Walter and Blobel, 1983). EKRM concentrations (in eq/μL) are calculated based on the concentration of the CRM preparation used, assuming 100% recovery of the vesicles (Walter and Blobel, 1983).

2.4.1 Pelleting assay for microsome association

Binding reactions were layered over a 100 μl sucrose cushion. The composition of the sucrose cushion was similar to the buffer composition of the binding reaction, but containing 0.5M sucrose. Following centrifugation at 20 psi for 10 min. in the A-100-30 rotor in a Beckman Airfuge, or 55000 rpm for 10 min. in the TLA 100 rotor in the Beckman TL-100 ultracentrifuge, the supernatant was fractionated into top (T) and middle (M) fractions of equal volume. The pellet (B) was resuspended in an equal volume of 50mM Tris-Cl, 1% SDS, pH9.0 and heated at 70°C for 10 min. These fractions were then processed for SDS-PAGE and visualized by western blotting.

2.4.2 Isolation of mitochondria

Mitochondria were isolated from tissue from a single rat liver as described in Greenawalt, 1974, except that the isolation medium (Buffer A) was composed of 2mM Hepes-KOH pH 7.4, 70mM sucrose, and 220mM mannitol. The crude mitochondria obtained were further purified by gradient centrifugation over a continuous 20%-40% Nycodenz gradient at 100000xg for 1 hr at 4°C. The lower of the two bands, containing the mitochondria, was collected through the side of the tube, washed once in Buffer A, and resuspended in 500 μL Buffer B (10mM Hepes-KOH pH 7.4, 250mM sucrose, 2mM

K_2HPO_4, 5mM sodium succinate, 1mM DTT, 1mM ATP, 0.08mM ADP). The concentration of total protein in the resuspension was determined by measuring A_{280} of 5 µL of mitochondria diluted to 1 mL with 0.1M NaOH ($A_{280}/0.00238$ = µg total protein/5 µL mitochondria). The mitochondria were then diluted with Buffer B containing 1 mg/mL fatty-acid free BSA to a final concentration of 4 mg total protein/mL.

2.4.3 Pelleting assay for association with mitochondria

Binding of Bcl-X_L to mitochondria was determined by a pelleting assay as described in Section 2.4.1, except that mitochondria were pelleted by centrifugation through the sucrose cushion for 10 min. at full speed in a benchtop microfuge at 4°C.

2.4.4 Production of large unilamellar vesicles (LUVs)

Lipids were dissolved in chloroform to a concentration of 10 mg/mL. Dissolved lipids were mixed in glass test tubes and the chloroform evaporated under a nitrogen stream. The resulting lipid films were placed under vacuum for two hours to remove all traces of solvent. Dried lipid films were placed under argon and stored at -20°C until needed. All lipid films were composed of 60% dioleoylphosphatidylcholine (DOPC) and 40% dioleoylphosphatidylglycerol (DOPG), except where indicated.

Lipid films were resuspended to a concentration of 1 mg/mL by vortexing in Buffer R. The lipid samples were subjected to 10 freeze-thaw cycles, followed by extrusion through a 0.1µm membrane (15 passes). Extruded LUVs were stored at 4°C under argon and used within 24 hours of extrusion. The total lipid concentration was

assumed to be 1 mg/mL, based on the assumption of 100% recovery of lipids following extrusion.

2.4.5 Flotation assay for binding to LUVs

Liposome/protein binding reactions were added to a sucrose buffer so that the final sucrose concentration was 1.4M sucrose in 200 μL. These samples were overlaid with 600 μL of 1.15M sucrose buffer, followed by 200 μL of 0.8M sucrose buffer. The composition of the sucrose buffers was similar to the buffer composition of the initial binding reaction, with sucrose added. The sucrose gradients were centrifuged at 356000xg for 3.5-4.5 hours at 18°C. Following centrifugation the samples were fractionated into four 250 μL fractions. The pellet was resuspended in 250 μL 50mM Tris-Cl pH 9.0, 1% SDS and incubated at room temperature for 20 min. Fractions were then processed for SDS-PAGE and visualized by western blotting (purified protein) or autoradiography (protein made by *in vitro* translation).

2.5 Labelling with IANBD

A ~20-fold molar excess of IANBD (from a 10mM stock solution dissolved in dimethylformamide) was added to Bcl-X_L in PS Elution Buffer. Generally, the concentration of Bcl-X_L was 4μM and the concentration of IANBD was 80μM in the labelling reaction. The reaction was incubated in the dark, with stirring, at room temperature for 2 hours, then quenched by the addition of 5mM DTT. The labelled Bcl-X_L was then separated from free dye by gel filtration over a 1.5 X 20 cm G-25 Sephadex

column. The protein was eluted from the column in G-25 Buffer.

2.5.1 Calculation of degree of labelling

The extent of labelling was calculated using the formula:

$$\frac{moles\ dye}{moles\ protein} = \frac{A_{478}}{\varepsilon_{478}} \times \frac{MW\ of\ protein}{mg\ protein/mL}$$

where A_{478} is the absorbance of the labelled sample at 478 nm (the absorption maximum wavelength of NBD), and ε_{478} is the molar extinction coefficient of NBD at 478 nm (given by Molecular Probes as 24,200 M^{-1} cm^{-1}). The protein concentration was determined as described in Section 2.3.1.

2.5.2 Acetone precipitation of NBD-labelled proteins

25 µg of protein in G-25 Buffer was added to 8 volumes of 100% acetone at -20°C, mixed, and allowed to precipitate overnight at -20°C. Precipitates were centrifuged 20 min at 3000xg (4°C). The acetone was removed by aspiration and the pellet was resuspended in 30 µL of Tricine Loading Buffer.

2.6 Steady-state fluorescence

All fluorescence measurements were carried out using a Model C-60SE Steady State Spectrofluorometer from Photon Technology International. The excitation wavelength was 478 nm. Slits were set at a width such that emission intensities fell

between 60,000 and 200,000 counts/sec (generally 2 to 4 nm) and kept constant throughout an experiment. Plastic cuvettes with a path length of 1 cm were used (DiaMed Lab Supplies Inc.). In all cases the net NBD intensity was determined by subtracting the signal of an equivalent sample lacking NBD-labelled protein. Intensity measurements were taken at room temperature. When liposome binding reactions were incubated at 37°C, the samples were cooled to room temperature for at least 20 min. before the intensity was measured again.

For the fluorescence experiments involving binding of NBD-labelled Bcl-X_L to EKRMs, the ratio of EKRMs (in eq) to Bcl-X_L (in μg) required for maximum binding of Bcl-X_L was determined for each EKRM preparation by titrating the amount of EKRMs present against a fixed amount of Bcl-X_L and measuring binding by pelleting assay. This ratio was then kept constant in all the fluorescence experiments using the same EKRM preparation. The ratio varied between 9 and 28 eq EKRMs/μg Bcl-X_L, depending on the EKRM preparation used.

2.6.1 CL2B filtration of EKRM-associated protein

.1 mL binding reactions were run over a 10 mL CL2B Sepharose column with a 1.5 cm diameter. Microsomes were eluted with Targeting Buffer. Drops 56-110, containing the microsomes, were collected and used for subsequent fluorometric analysis.

An equivalent sample containing microsomes only was treated identically to the sample containing microsomes and NBD-X_L, to provide a blank signal for determining NBD-intensity.

2.6.2 Iodide quenching

NBD-containing and blank samples were each split into two equivalent 1 mL samples. One of each pair was adjusted to 0.2M KI using a stock solution of 4M KI, 1mM $Na_2S_2O_3$. The other was adjusted to 0.2M KCl using a stock solution of 4M KCl, 1mM $Na_2S_2O_3$. The initial intensity (Fo) of the sample containing KCl was determined, and then the sample containing KI was titrated into the sample containing KCl. The fluorescence intensity was redetermined following each addition.

Iodide quenching data was analyzed according to the Stern-Volmer law:

$$\frac{Fo}{F} - 1 = Ksv[I^-]$$

where Fo is the net emission intensity in the absence of I^-, F is the net emission intensity in the presence of I^-, and Ksv is the Stern-Volmer quenching constant.

2.6.3 Quenching with lipophilic quenchers

LUVs containing 0%, 10%, 20% and 30% 1-palmitoyl-2-stearoyl-(7-doxyl)-phosphatidylcholine (7-NO-PC) were produced as described in Section 2.4.4, except lipid films were resuspended at a concentration of 2 mg/mL. DOPG was kept constant at 40% and DOPC made up the balance of the lipids. 92nM aliquots of NBD-X_L were mixed with each type of liposome at a concentration of 1.3mM total lipid (assuming 100% recovery of lipids following extrusion). The emission intensity of NBD-X_L was determined immediately after mixing. The samples were then incubated 3 hours at 37°C, cooled back to room temperature, and the intensities were remeasured. Slit widths for these intensity

readings were 6 nm. The fluorescence intensities following binding were normalized to the initial intensities to account for any differences in the NBD-X_L content in each sample. F/Fo for each sample was calculated, where F was the normalized NBD intensity in the 7-NO-PC containing samples and Fo was the normalized NBD intensity in the sample lacking 7-NO-PC.

2.7 Quantitative western blotting

Western blots were run as described in Section 2.2. An image of the developed blot was taken using the Kodak Image Station (MOBIX). The net band intensities were quantified using the associated Image Analysis software. Serial dilutions of known amounts of NBD-X_L were run on the same gel as the unknowns to act as standards. Band intensity measurements of the standards were used to construct a NBD-X_L standard curve and the amount present of each unknown was determined from this curve.

For the quantitative western blots of flotation assay fractions rabbit α-Bcl-X_L primary antibody was used at a dilution of 1:6667.

2.8 Statistical calculations

Mean values ($\bar{x}$) for n replicate samples were calculated as follows:

$$\bar{x} = \frac{\Sigma x}{n}$$

Standard error of the mean (*s.e.m.*) for mean values was calculated as follows:

$$s.e.m. = \sqrt{\frac{\Sigma (x - \bar{x})^2}{n(n - 1)}}$$

Where a value was obtained from the average of only two measurements, the error is given by the deviation (D) of the two measurements from the average value:

$$D = |x - \bar{x}|$$

Chapter 3: Results

3.1 Expression and purification of human Bcl-X_L

Much of the published experimental work on Bcl-X_L uses a truncated version of the protein lacking its hydrophobic C-terminal sequence. This is due to difficulty obtaining recombinant full-length protein that is soluble in the bacteria. The presence of the insertion sequence will cause binding of the protein to the bacterial plasma membrane. To get around this problem the IMPACT™ (Intein Mediated Purification with an Affinity Chitin-binding Tag) system from New England Biolabs was used. This system involves fusion of the C-terminus of the target protein (Bcl-X_L) to a protein splicing element from yeast known as an intein. The intein is in turn fused at its C-terminus to a chitin binding domain (CBD) which allows purification of the fusion protein over a chitin column. The intein has been engineered to undergo a self-cleavage reaction at its N-terminus when induced by the presence of nucleophilic agents such as hydroxylamine. Following the cleavage reaction Bcl-X_L is free to be washed from the column, leaving the intein-CBD moiety still bound to the chitin beads. The advantage of this system over others that create N-terminal fusions to the target protein is that it places the C-terminal hydrophobic sequence of Bcl-X_L in the center of the fusion protein where it is largely masked from aggregating with bacterial membranes or other hydrophobic proteins. Furthermore the intein-CBD affinity tag used for purification is specifically

removed from the purified Bcl-X_L.

Human Bcl-X_L was expressed and purified as described in Section 2.3. The purification yielded a relatively pure protein approximately the correct size for Bcl-X_L (Figure 4B).

It should be noted that some of the membrane binding studies subsequently described were done with protein that had not been purified over the phenyl Sepharose column (Figure 4A). No differences have been noted between those results and later results obtained with fully purified Bcl-X_L.

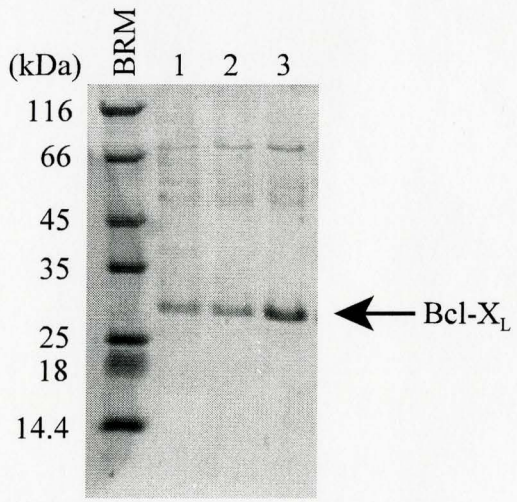

Figure 4A: Partial purification of full-length Bcl-X_L.
Coomassie Blue stained SDS-PAGE gel of recombinant Bcl-X_L eluted from three chitin columns run in parallel, as described in Section 2.3. 40 mL were eluted from each of the three columns, and 10 μL of each eluate was run on the gel (lanes 1-3). Sizes (in kDa) of the broad range markers (BRM) are indicated on the left.

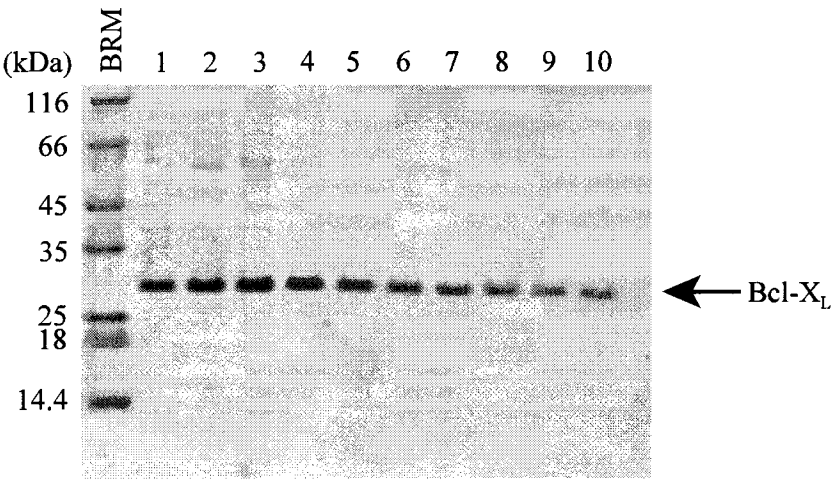

Figure 4B: Final purification of full-length Bcl-X_L.
Coomassie Blue stained SDS-PAGE gel of purified Bcl-X_L. The eluates from each column in Figure 4A were combined and run over a phenyl Sepharose column as described in Section 2.3. Fractions (2 mL each) containing Bcl-X_L were eluted from the phenyl Sepharose column with PS Elution Buffer. 10 μL of each fraction was run on the gel (lanes 1-10). These fractions were combined and used for subsequent studies on Bcl-X_L. Sizes (in kDa) of the broad range markers (BRM) are indicated on the left.

3.2 Binding of recombinant Bcl-X_L to membranes

Due to the hydrophobic nature of Bcl-X_L, the recombinant protein proved to be very difficult to work with, as it has a tendency to aggregate and adhere to surfaces. For this reason, Bcl-X_L is purified in the presence of the zwitterionic detergent 3-[(3-cholamidopropyl)dimethylammonio]-1-propane sulfonate (CHAPS). CHAPS has a relatively high critical micelle concentration (cmc) of 0.4% (w/v), which means enough CHAPS can be added to the purification procedure to keep Bcl-X_L soluble without the

detergent forming micelles which could destroy biological membranes during subsequent membrane-binding experiments.

The effect of CHAPS on dog pancreatic ER microsomes (CRMs) was characterized to determine appropriate conditions for attempting to bind Bcl-X_L to CRMs. Calreticulin is a lumenal ER protein, and substantial leakage caused by incubation in CHAPS would indicate a loss of membrane integrity. Microsomes were incubated in the presence of varying concentrations of CHAPS (lower than the cmc), and then subjected to the standard membrane pelleting procedure (explained in Section 2.4.1). Top, middle and bottom fractions were probed for the presence of calreticulin by western blot (Figure 5A). A fraction of the calreticulin is found outside of the lumen even in the absence of detergent, as evidenced by the presence of calreticulin in both the top and bottom fractions. This may be due to the isolation procedure for CRMs. Concentrations of CHAPS up to 0.015% do not appear to alter the amount of calreticulin found in both fractions. A slight increase in the amount of calreticulin in the top fraction can be detected at 0.02% and above. Release of calreticulin is complete at 0.06%, or possibly lower since the sample incubated at 0.045% did not transfer properly to nitrocellulose.

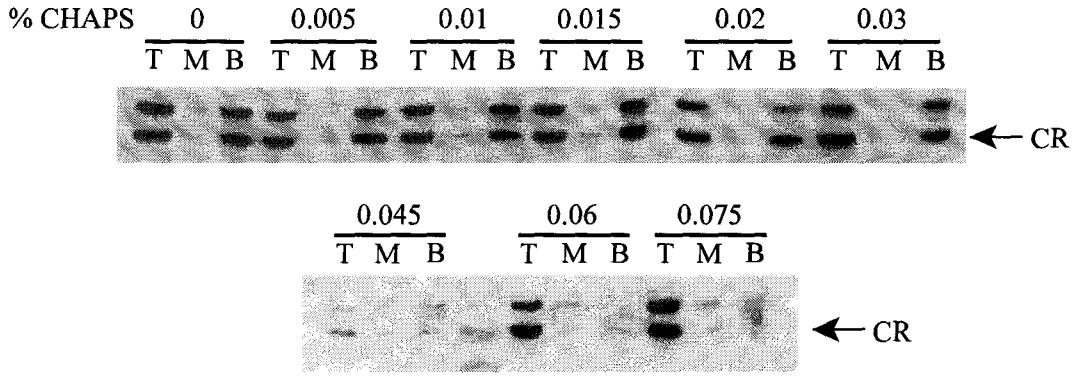

Figure 5A: Calreticulin retention in CHAPS.
CRMs (0.18 eq/μL) were incubated in Targeting Buffer containing the indicated amounts of CHAPS for 1 hour at 24°C, then subjected to the membrane pelleting assay as described in Section 2.4.1. Calreticulin (CR) was detected by western blot.

Membrane viability was also tested by the ability of the membranes to carry out signal sequence cleavage and glycosylation. Both of these activities require the presence of a functional SRP receptor and translocon, components necessary for classical SRP-dependent membrane targeting. Preprolactin is processed to its mature form, prolactin, by cleavage of its N-terminal signal sequence upon translocation. This results in a slight shift downwards in mobility upon SDS-PAGE electrophoresis. A functional mutant of the transmembrane beta subunit of SRP receptor (Srβ) containing two glycosylation sites was used to test glycosylation activity. Glycosylation causes a shift upwards in mobility

upon SDS-PAGE electrophoresis. CRMs retain both signal sequence cleavage and glycosylation activities in 0.015% CHAPS (Figure 5B). Based on the combined results of Figures 5A and 5B the concentration of CHAPS in all membrane binding reactions was kept at 0.015%.

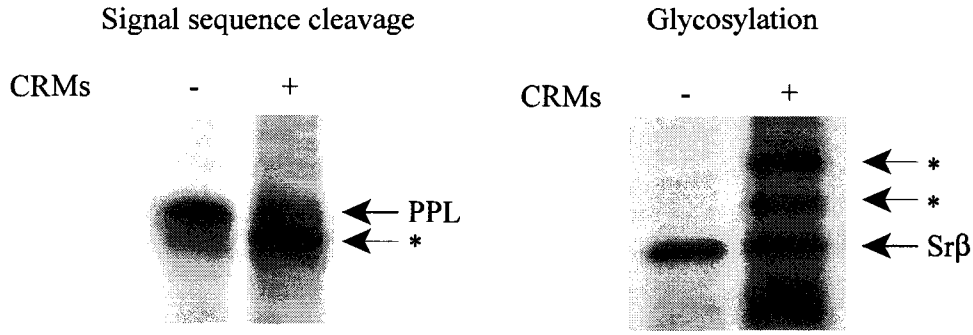

Figure 5B: **Signal sequence cleavage and glycosylation in CHAPS.**
(left) Preprolactin produced by *in vitro* translation was incubated cotranslationally with 1.8 eq of CRMs (+), or translated in the absence of CRMs (-) for 1 hour at 24°C. All translation reaction volumes were 10 μL. Full-length preprolactin (PPL) and signal-cleaved prolactin (*) are indicated. Proteins were detected by autoradiography.

(right) Modified Srβ produced by *in vitro* translation was incubated cotranslationally with 1.8 eq of CRMs (+), or translated in the absence of CRMs (-) for 1 hour at 24°C. All translation reaction volumes were 10 μL. Unglycosylated Srβ and the glycosylated forms of Srβ (*) are indicated. Proteins were detected by autoradiography.

3.2.1 Binding of Bcl-X_L to ER microsomes

When Bcl-X_L was incubated with microsomes in 0.015% CHAPS it appeared in the bottom fraction of the pelleting assay, indicating association with the microsomes (Figure 6). In the absence of microsomes Bcl-X_L was soluble and therefore remained in the top fraction of the pelleting assay. Binding of Bcl-X_L to microsomes did not appear to increase the amount of calreticulin appearing in the top fraction, indicating that the protein was not adversely affecting the integrity of the membranes (compare Figure 5A and Figure 6). Bcl-X_L can also bind to EKRMs, which are column-washed and EDTA- and salt-extracted CRMs (Walter and Blobel, 1983). The extraction of CRMs with salt and EDTA removes peripheral proteins and most ribosomes from the membranes, reducing the optical density of the membranes considerably and causing less light scatter in fluorometric experiments. No difference in binding of Bcl-X_L was seen between CRMs and EKRMs (data not shown). Occasionally 100 μg/mL BSA was included in the binding reaction to increase solubility/stability of the protein in the absence of membranes, but this did not affect the binding of Bcl-X_L to membranes.

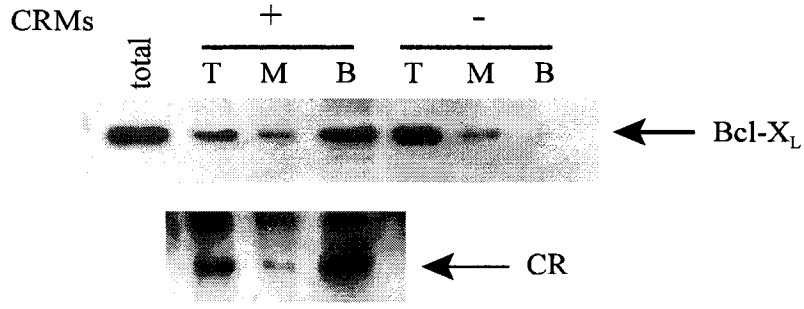

Figure 6: **Binding of Bcl-X_L to microsomes in the presence of 0.015% CHAPS.** Purified Bcl-X_L (0.26μM) in Targeting buffer + 100 μg/mL BSA was incubated in the presence (+) or absence (-) of CRMs (0.12 eq/μL) for 1 hour at 24°C. Incubations were subjected to the membrane pelleting procedure described in Section 2.4.1. Lane 1 shows the total amount of Bcl-X_L input. The T, M, and B fractions from the sample containing CRMs were also assayed for the presence of calreticulin (CR) (lower panel). All proteins were detected by western blot.

3.2.2 Binding of Bcl-X_L to mitochondria

Some attempts were also made to bind Bcl-X_L to mitochondria isolated from rat liver. Mitochondrial integrity was measured as the ability to import the fusion protein pOCTgPA, and the ability to retain cytochrome c within the intermembrane space. pOCTgPA contains the N-terminal signal peptide and first 29 amino acids of the rat mitochondrial matrix protein preornithine carbamoyltransferase, fused to the passenger protein gPA (Janiak *et al.*, 1994b). The translocation of pOCTgPA requires an electrochemical gradient across the inner mitochondrial membrane. Some pOCTgPA

import could be seen only at the highest concentration of mitochondria, indicating the translocation was inefficient (Figure 7). Cytochrome c was difficult to detect by western blot, but could be seen at the highest concentration of mitochondria, colocalizing with the mitochondrial marker hsp60 (a matrix protein) in the bottom fraction. The band that appears in the top fraction in the hsp60 panel is presumably a contaminating protein from the Bcl-X_L preparation that cross-reacts with hsp60 antibody, since it appears even in the absence of mitochondria. Purified Bcl-X_L did not show any appreciable binding to mitochondria. Cytochrome b5 synthesized by *in vitro* translation (cb5) was used as a binding control since it inserts into virtually any bilayer *in vitro* (Kim *et al.*, 1997). In contrast to Bcl-X_L, cytochrome b5 was capable of binding to the mitochondria. Due to the difficulty in working with purified rat liver mitochondria, and since successful binding to one intracellular membrane had already been achieved, further work on this aspect of Bcl-X_L was set aside to focus on the fluorescence experiments that were the main goal of my project.

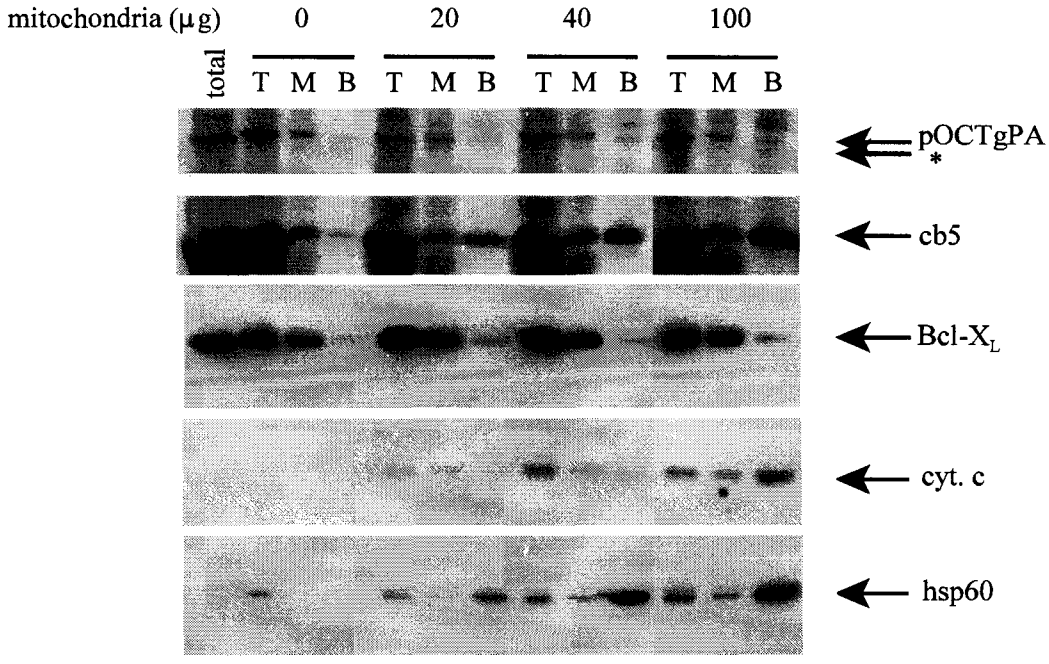

Figure 7: **Binding of Bcl-X_L to purified rat liver mitochondria.** pOCTgPA and cytochrome b5 (cb5) produced by *in vitro* translation (7 μL of each translation reaction), and purified Bcl-X_L (0.59μM), were incubated with purified rat liver mitochondria for 1 hour at 30°C. The amount of mitochondria (in μg total protein) used in each reaction is indicated. The binding reactions were then subjected to a membrane pelleting assay as described in Section 2.4.3. The samples containing Bcl-X_L were also probed for the presence of hsp60 and cytochrome c (cyt. c). The cleaved form of pOCTgPA is indicated by *. Lane 1 of the top three panels is the total amount of protein input into each reaction. pOCTgPA and cytochrome b5 were detected by autoradiography, Bcl-X_L, cytochrome c and hsp60 were detected by western blot.

3.2.3 Binding of Bcl-X_L to liposomes

Published studies have shown that Bcl-X_L will bind to liposomes composed of dioleoylphosphatidylcholine (DOPC) and dioleoylphosphatidylglycerol (DOPG) in ratios of 60 to 40 mol % (Basañez *et al.*, 2001). Large unilamellar vesicles (LUVs) composed of 60% DOPC and 40% DOPG were generated as described in Section 2.4.4. Flotation assays (see Section 2.4.5) were used to assess the liposome-binding of NBD-X_L. During equilibrium centrifugation liposomes and any associated protein will float to the top of the sucrose gradient and be found in fractions 1 and 2, while free protein will remain mainly in fractions 3, 4 and 5. Figure 8A shows that the liposomes are competent to bind cytochrome b5, and that 0.015% CHAPS added at the beginning of the incubation period does not appear to affect this binding significantly (Figure 8A, compare left and right panels). When Bcl-X_L was incubated with liposomes a fraction of the protein molecules bound to the liposomes (Figure 8B).

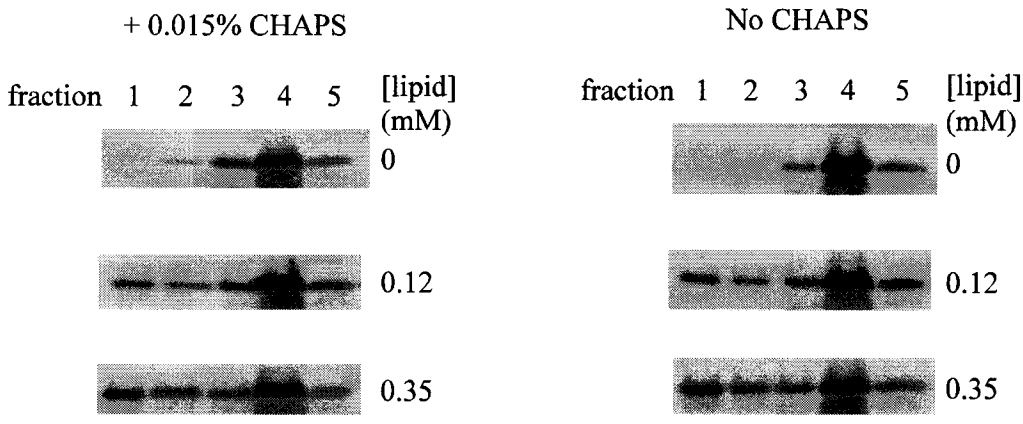

Figure 8A: Binding of cytochrome b5 to liposomes.
Cytochrome b5 produced by *in vitro* translation (40 µL of translation reaction) was incubated post-translationally with large unilamellar vesicles (LUVs) for 3 hours at 24°C. The total lipid concentration in each sample is indicated to the right of each panel. The samples were then subjected to a flotation assay as described in Section 2.4.5. Flotation assay fractions are indicated, with fraction 1 being the top of the sucrose gradient, fraction 4 being the bottom of the gradient, and fraction 5 being the resuspended pellet. Cytochrome b5 was detected by autoradiography.

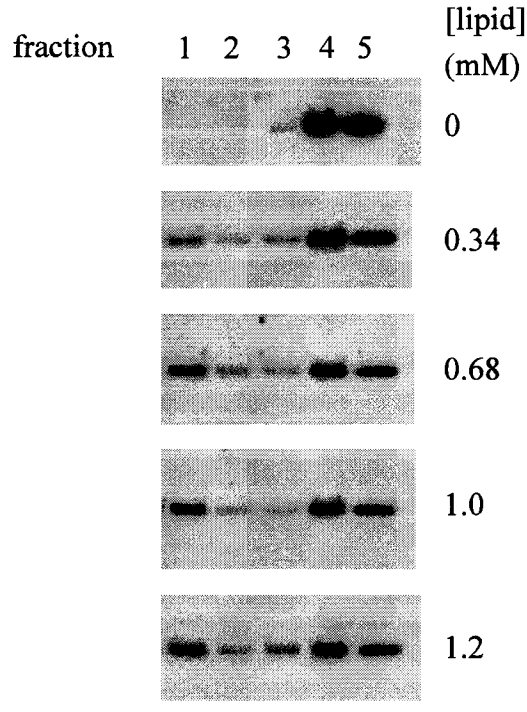

Figure 8B: **Binding of Bcl-X_L to liposomes.**
Purified Bcl-X_L (92nM) was incubated with LUVs for 3 hours at 37°C. The total lipid concentration in each sample is indicated to the right of each panel. The samples were then treated as described in the caption of Figure 8A. Bcl-X_L was detected by western blot.

3.3 Labelling of Bcl-X_L with IANBD

The fluorophore used to label Cys151 of Bcl-X_L was *N*,*N'*-dimethyl-*N*-(iodoacetyl)-*N'*-(7-nitrobenz-2-oxa-1,3-diazolyl)ethylenediamine (IANBD) (Figure 9A). This iodoacetamide derivative of NBD reacts with free nucleophiles such as sulfhydril groups (Figure 9B) and therefore specifically labels cysteines under controlled pH and reaction time.

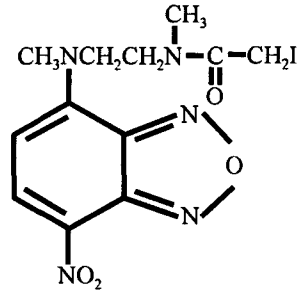

Figure 9A: The chemical structure of IANBD.

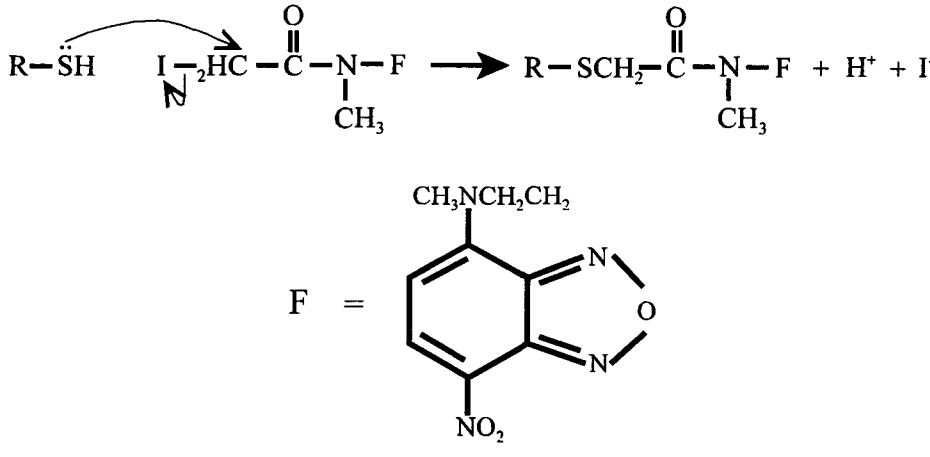

Figure 9B: Reaction of IANBD with sulfhydril groups.

NBD is an environmentally sensitive fluorescent molecule whose emission intensity can increase significantly (>3 times) when it moves from an aqueous to a hydrophobic environment (Shepard *et al.*, 1998). The peak emission wavelength is also blue-shifted by several nm in a hydrophobic environment. This property of NBD was confirmed by measuring its fluorescence spectrum in a variety of buffers of different hydrophobicity (Figure 10). In water NBD gives a very broad peak, with the peak maximum centered around 542 nm, the same wavelength as the published maximum for this dye in methanol. The buffer used for binding reactions (Targeting Buffer) does not significantly affect the signal of NBD relative to its signal in water. However, 1% Triton-X100 increased the signal by 3 times, and blue-shifted the peak by roughly 10 nm, to a maximum of approximately 535 nm. 10% Triton-X100 increased the signal even further, and shifted the peak to a lower wavelength by 2 or 3 nm (Figure 10).

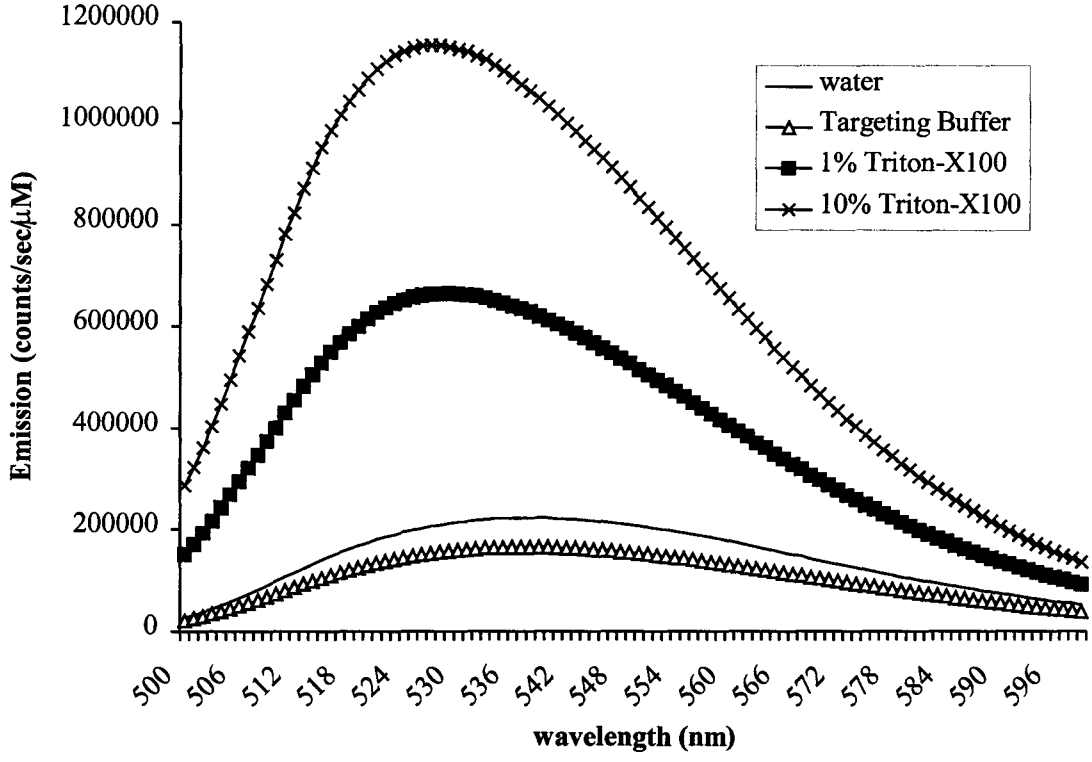

Figure 10: Fluorescence signal from free IANBD in buffers of differing hydrophobicity.
Spectra of 1 μM IANBD in water, Targeting Buffer, 1% Triton-X100, or 10% Triton-X100 were taken in a fluorometer as described in Section 2.6.

Labelling of Bcl-X_L was carried out as described in Section 2.5. To test for labelling specificity a Bcl-X_L mutant with its sole cysteine, Cys151, mutated to serine (Bcl-C151S) was constructed. Bcl-X_L and Bcl-C151S were expressed and purified by the same methods and were labelled in parallel under the same conditions and using the same stock solution of IANBD, as described in Section 2.5. The extent of labelling of Bcl-X_L with IANBD, calculated as described in Section 2.5.1, was 0.58 dye molecules/protein, while for Bcl-C151S it was 0.55 dye molecules/protein. Spectra were taken of each protein and the emission intensities were normalized to the concentration of NBD present. The signal per unit NBD concentration of NBD-C151S was considerably lower than that of NBD-X_L (Figure 11). Therefore the NBD associated with Bcl-C151S is in a different environment than the NBD attached to Bcl-X_L.

The emission peak of NBD attached to Bcl-X_L is approximately 530 nm. As shown in Figure 10, the free NBD molecule in solution displays an emission peak at 542 nm, which corresponds to the published value for this dye in methanol. This implies that in the soluble protein the local environment surrounding Cys151 is quite hydrophobic, evidence that is supported by the crystal structure of the protein which places this cysteine in the centre of a bundle of α-helices (see Figure 3).

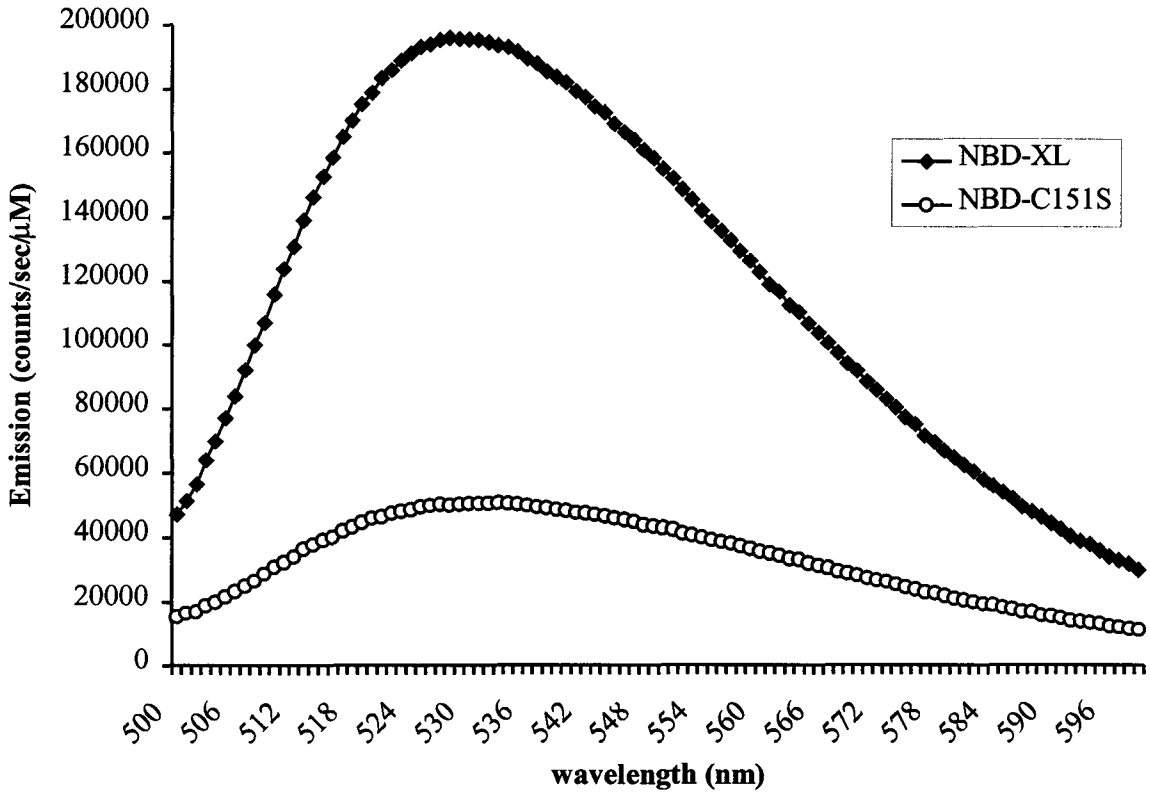

Figure 11: **Spectra of NBD-labelled Bcl-X_L and Bcl-C151S.**
Spectra of NBD-X_L and NBD-C151S were taken in a fluorometer, as described in Section 2.6. The results are displayed as the emission per unit concentration of NBD in the cuvette. The concentration of NBD was determined by absorption spectrophotometry (A_{478} = 0.030 and 0.033 for NBD-X_L and NBD-C151S respectively) using an extinction coefficient of 24,200 cm^{-1} M^{-1}.

In order to confirm that Bcl-X_L was the primary fluorescent product, and that it was covalently labelled with NBD, the purity of each of the NBD-labelled proteins was determined by separation by SDS-PAGE. Following electrophoresis the gel was soaked in DMSO to maximize the fluorescence intensity of the NBD. Although there are equivalent amounts of each protein present (Figure 12 upper), only Bcl-X_L is covalently labelled with NBD (Figure 12 lower). This indicates that NBD reacts covalently only with Cys151 under the conditions used, as opposed to amines for example. Binding of NBD to Bcl-C151S is non-covalent.

Following labelling, the protein was tested to make sure it retained the ability to bind to microsomes. As can be seen in Figure 13, NBD-labelled Bcl-X_L (NBD-X_L) behaves similarly to unlabelled Bcl-X_L regarding its ability to bind to CRMs (compare Figure 13 to Figure 6).

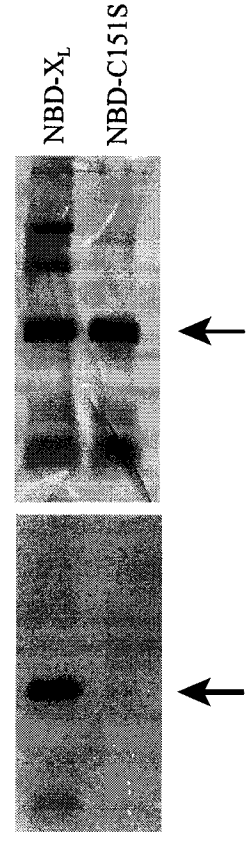

Figure 12: **Visualization of fluorescently-labelled proteins.**
Equal amounts of NBD-labelled Bcl-X_L and Bcl-C151S (NBD-X_L and NBD-C151S) were precipitated in acetone and run on an SDS-PAGE gel. Following electrophoresis the gel was soaked in DMSO and then illuminated with blue light from a filtered lightbox. Fluorescing proteins were seen through an orange filter. The same gel was then stained with Coomassie Blue to visualize all proteins present.

(upper panel) Gel stained with Coomassie Blue. The arrow indicates NBD-X_L/NBD-C151S.

(lower panel) Image of fluorescing proteins. The arrow indicates NBD-X_L/NBD-C151S.

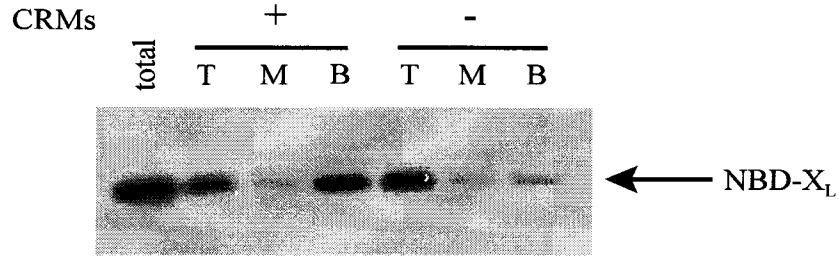

Figure 13: **Binding of NBD-X_L to microsomes.**
NBD-X_L (0.20μM) in Targeting buffer + 100 μg/mL BSA was incubated in the presence (+) or absence (-) of CRMs (0.12 eq/μL) for 1 hour at 24°C. Incubations were subjected to the membrane pelleting procedure described in Section 2.4.1. Lane 1 shows the total NBD-X_L input into the reaction. NBD-X_L was detected by western blot.

3.4 Steady-state fluorometry

When the emission of NBD-X_L following incubation with EKRMs is compared to the emission prior to incubation (Figure 14), it can be seen that there is only a very slight increase in intensity (approximately 20%), and this increase is dependent on the presence of membranes. The data in Figure 14 is the result of 7 independent experiments using 5 different preparations of NBD-X_L and 2 different preparations of EKRMs. The emission intensity is expressed as the ratio of intensity after incubation to intensity before incubation in each experiment. This removes the need to account for such factors as the

differing labelling efficiencies of each batch of labelled protein, different slit widths used, or other machine-associated parameters such as possible differences in the lamp intensity from experiment to experiment.

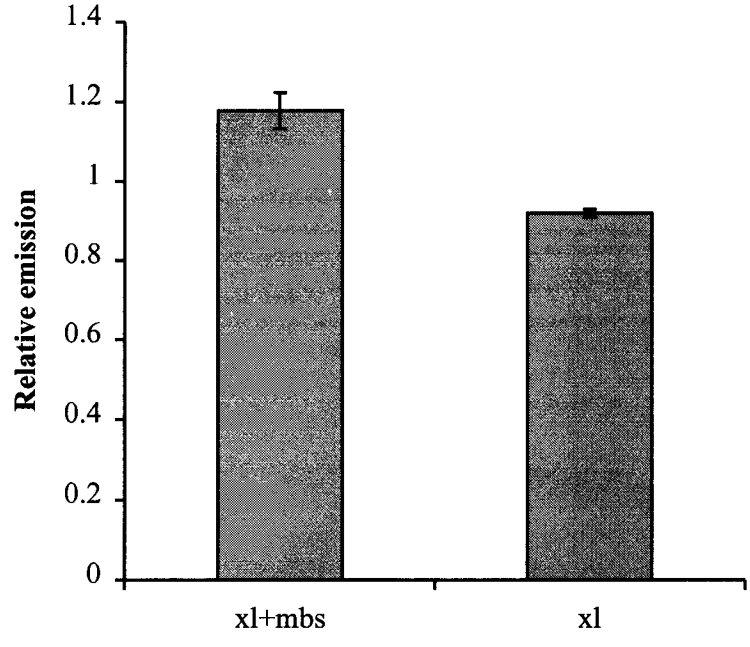

Figure 14: Comparison of the relative emission intensity at 530 nm of membrane-bound and free NBD-X_L.
NBD-X_L was added to EKRMs in Targeting Buffer (xl+mbs) or diluted in Targeting Buffer alone (xl) and the emission intensity at 530 nm was measured immediately, as described in Section 2.6. Following this measurement the two reactions were incubated for 1 hour at 24°C to allow binding to occur. The emission intensities were then remeasured. The relative emission intensity is the ratio of the final emission intensity (after incubation) to the initial emission intensity (before incubation). Each column represents the mean relative emission intensity (n=7). Error bars represent the standard error of the mean.

The small increase seen in NBD emission intensity upon membrane binding is much less than the increase of 3 times or more expected if the NBD was moving from an aqueous to a hydrophobic environment. Binding of recombinant Bcl-X_L to microsomes does not go to completion, presumably due to misfolding of a certain fraction of the protein. Emission intensity experiments average the signal from all NBD-X_L molecules, and there are at least two populations of NBD-X_L present, membrane-bound and unbound. An attempt was made to determine if the signal from the unbound population was masking larger alterations in the signal from the bound population. Membranes and any associated proteins can be separated from free protein by gel filtration over a CL2B Sepharose column, which has an exclusion limit of 40,000 kDa. Figure 15 shows an example of this type of gel filtration. EKRMs and bound NBD-X_L elute in fractions 2, 3, and 4 which constitute the void volume, while unbound NBD-X_L elutes primarily in the later fractions. Membrane-bound NBD-X_L samples were filtered over a CL2B Sepharose column as shown in Figure 15 and an emission spectrum was taken of the combined fractions indicated by the bracket. This spectrum was compared to the emission spectrum of a roughly equivalent concentration of NBD-X_L in the absence of membranes. In order to make this comparison the concentration of NBD-X_L in the two samples must be accurately determined. An attempt was made to do this by quantitative western blotting (as described in Section 2.7). Unfortunately it proved to be very difficult to get consistent results by this method. The samples had to be diluted between 50 and 100 times to bring them within the linear range of the chemiluminescence signal, potentially allowing pipet error to affect the results. In addition, loss of some purified protein due to adherence to

plastic surfaces was observed on several occasions (in spite of the detergent present). This loss was generally more pronounced for NBD-X_L alone than for NBD-X_L in the presence of membranes, possibly since the membranes provide an alternate surface for the protein to bind to. This could result in a systematic overestimation of the amount of protein present in the membrane-bound NBD-X_L sample compared to the amount in the free NBD-X_L sample. For whatever reason, repeated attempts at quantitative western blotting of these particular samples gave inconsistent and imprecise results and therefore the data from this experiment was considered unreliable and is not included here.

Another potential source of error in this experiment could come from the treatment of the blank sample. The blank, containing only microsomes, was eluted from the CL2B sepharose column in a manner identical to the sample containing NBD-X_L and microsomes. However, the signal to noise ratio was such that a 10% variation in the signal from the blank would cause a 10-15% difference in the blank-subtracted signal from the NBD-X_L. Therefore small differences in the concentration of microsomes between the blank and NBD-X_L-containing samples could cause a similar degree of error in the net emission intensity measured following CL2B filtration.

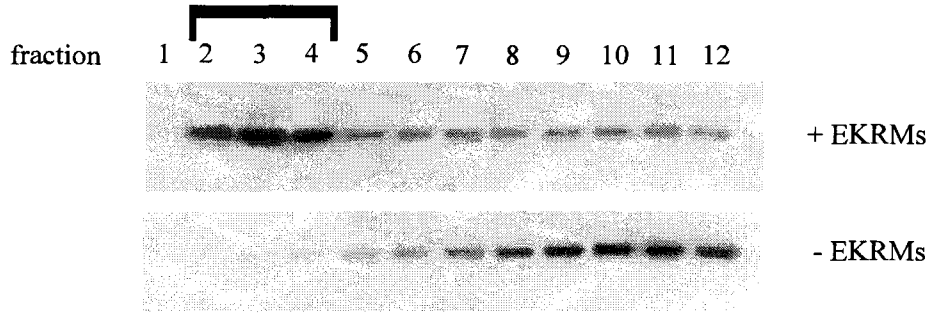

Figure 15: Separation of NBD-X_L bound to EKRMs from free NBD-X_L. NBD-X_L (1.2μM) incubated for 1 hour at 24°C with (top) or without (bottom) EKRMs (0.27 eq/μL), in a total volume of 1 mL, was run over a CL2B Sepharose column with a bed volume of 10 mL. The column was equilibrated and eluted with Targeting Buffer. Fractions of 15 drops were collected. 1 μL of each fraction was run on an SDS-PAGE gel and NBD-X_L was detected by western blot. The fractions containing NBD-X_L bound to EKRMs (indicated by the bracket) are kept for fluorometric analysis as described in the text and in Section 2.6.1.

Unlike the results obtained with EKRMs (Figure 14), incubating NBD-X_L with liposomes (60% DOPC, 40% DOPG) does result in a significant increase in the emission intensity (Figure 16). The increase was not due to the increased incubation temperature (37°C vs. 24°C with EKRMs) since incubating NBD-X_L with EKRMs at 37°C for 3 hours did not produce results significantly different from those seen in Figure 14 (data not shown).

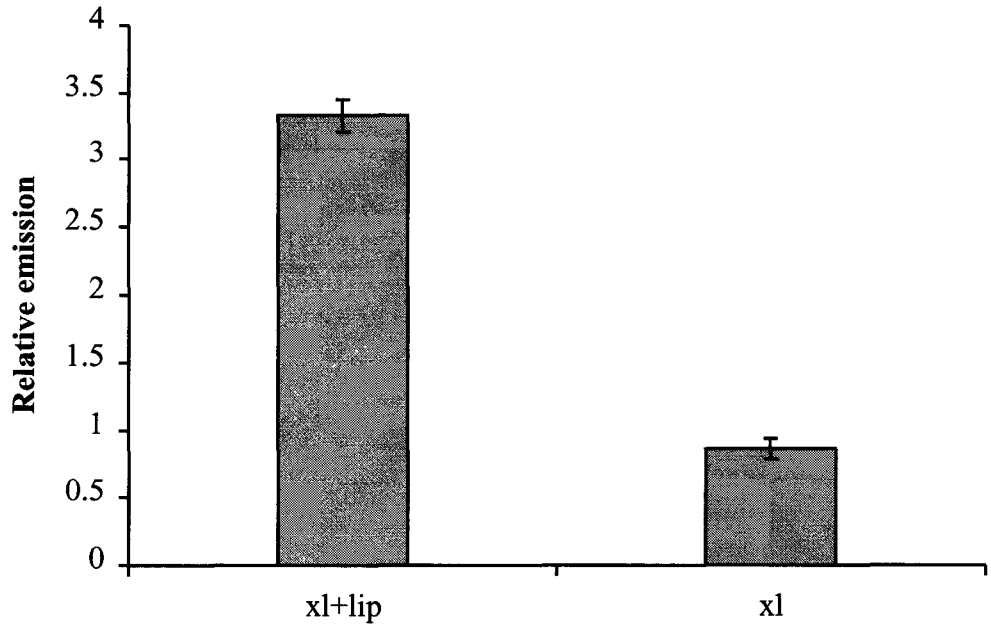

Figure 16: **Comparison of the relative emission intensity at 530 nm of liposome-bound and free NBD-X_L.**
NBD-X_L (92nM) was added to liposomes (1.3mM total lipid) in Buffer R containing 0.015% CHAPS (xl+lip) or diluted in this buffer alone (xl) and the emission intensity at 530 nm was measured immediately. Following this measurement the two samples were incubated for 3 hours at 37°C to allow binding to occur. The emission intensities were then remeasured. The relative emission intensity is the ratio of the final emission intensity (after incubation) to the initial emission intensity (before incubation). Each column represents the mean relative emission intensity (n=3). Error bars represent the standard error of the mean.

3.4.1 Iodide quenching

To further investigate the location of Cys151 upon binding of Bcl-X_L to membranes the accessibility of Cys151 to aqueous quenchers was assayed. In collisional quenching a quencher contacts a fluorophore during the lifetime of the excited state and returns it to the ground state without emission of a photon, resulting in a decrease in emission intensity (Lakowicz, 1999). The requirement for contact between fluorophore and quencher makes collisional quenching useful for studying the accessibility of the fluorophore to the quencher. A decreased degree of quenching by an aqueous quencher, such as iodide ions, would indicate the fluorophore was in an environment unavailable to the quencher, such as the interior of the membrane bilayer

Collisional quenching can be described by the Stern-Volmer equation,

$$\frac{Fo}{F} - 1 = Ksv\,[Q]$$

where Fo is the fluorescence intensity in the absence of quencher, F is the intensity in the presence of quencher, and [Q] is the concentration of quencher. Plotting Fo/F-1 versus [Q] ideally gives a straight line with the slope equal to Ksv, the Stern-Volmer quenching constant. Ksv is indicative of the degree of quenching, a more quenchable species will have a higher Ksv in a Stern-Volmer plot.

A sample of NBD-X_L bound to EKRMs (separated from free NBD-X_L by CL2B Sepharose filtration) and a sample of free NBD-X_L were quenched with KI as described in Section 2.6.2. Figure 17 shows a representative Stern-Volmer plot for these two samples. Both show a linear relationship between Fo/F-1 and quencher concentration, as would be expected with a collisional quenching mechanism.

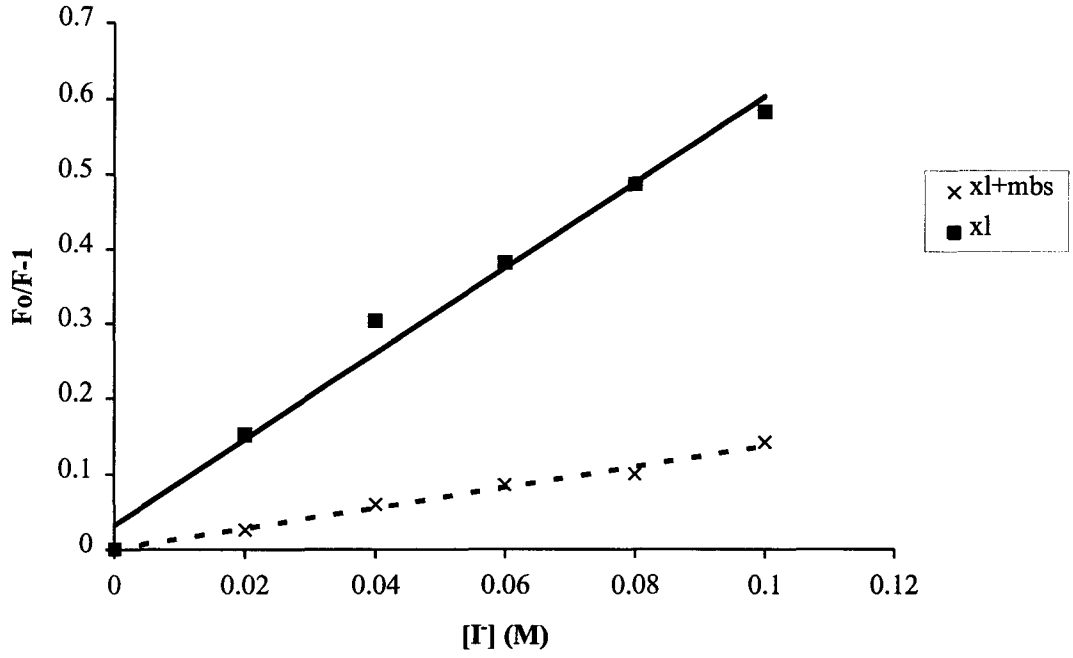

Figure 17: **Iodide quenching of NBD-X_L in the presence and absence of EKRMs.** Stern-Volmer plots of NBD-X_L bound to EKRMs (xl+mbs) and free NBD-X_L (xl) quenched by iodide ions.

The average Ksv values for EKRM-bound NBD-X_L and free NBD-X_L are 1.3 ± 0.1 M^{-1} (n=2, uncertainty is the deviation from the mean) and 7.0 ± 0.7 M^{-1} (n=6, uncertainty is the standard error of the mean) respectively. Changing the signal given by the blank by 10% only produces a 2% difference in the calculated Ksv values. Therefore, unlike the net emission intensity measurements, small differences in the EKRM concentration between the sample and the blank should not significantly affect the results given here. According to this data, Cys151 is less accessible to aqueous quenchers when NBD-X_L is bound to membranes, than when NBD-X_L is free in solution.

Iodide quenching was also carried out on NBD-X_L bound to liposomes, although in this case the liposomes were not separated from any free NBD-X_L present. The average Ksv (n=2) of liposome-bound NBD-X_L was 3.9 ± 0.3 M^{-1} (uncertainty is the deviation from the mean). Interestingly, in these two experiments the average percentage of the fluorescence quenched by 0.1M iodide was 29 ± 3% for NBD-X_L incubated with liposomes, while for free NBD-X_L it was 47 ± 4% (percentage of fluorescence quenched = (1-F/Fo) x 100%). This appears to indicate that 0.1M iodide was roughly 62% as effective at quenching NBD-X_L incubated with liposomes versus free NBD-X_L, implying that approximately 38% of the NBD-X_L in the liposome/NBD-X_L mixture is protected from quenching.

3.4.2 Quenching by lipophilic quenching agents

The decreased degree of iodide quenching seen for NBD-X_L bound to membranes suggests that Cys151 is in fact inserted into the bilayer. This can be confirmed by using quenching agents that are restricted to the interior of the membrane bilayer. 1-palmitoyl-2-stearoyl-(7-doxyl)-phosphatidylcholine (7-NO-PC) contains a nitroxide group attached to one of the acyl chains, which serves as a quencher. Placing the quencher group at the 7 position puts it in the center of one leaflet of the bilayer. From this position it can contact and quench a NBD group positioned anywhere within the bilayer (Shepard *et al.*, 1998). Liposomes were loaded with various concentrations of 7-NO-PC and the emission intensity of NBD-X_L following incubation with these liposomes was compared to the emission of NBD-X_L incubated with liposomes lacking the quencher.

Lipophilic quenching experiments were carried out as described in Section 2.6.3. Figure 18 shows the relative decrease in emission intensity of NBD-X_L incubated with liposomes containing 10, 20, and 30% 7-NO-PC. There is a steady decrease in fluorescence with increasing quencher concentration. Approximately 25% of the fluorescence is quenched by the maximum quencher concentration of 30% 7-NO-PC. The 7-NO-PC quenching data was not plotted according to the Stern-Volmer equation because this type of quenching involves a significant static quenching component (Shepard *et al.*, 1998).

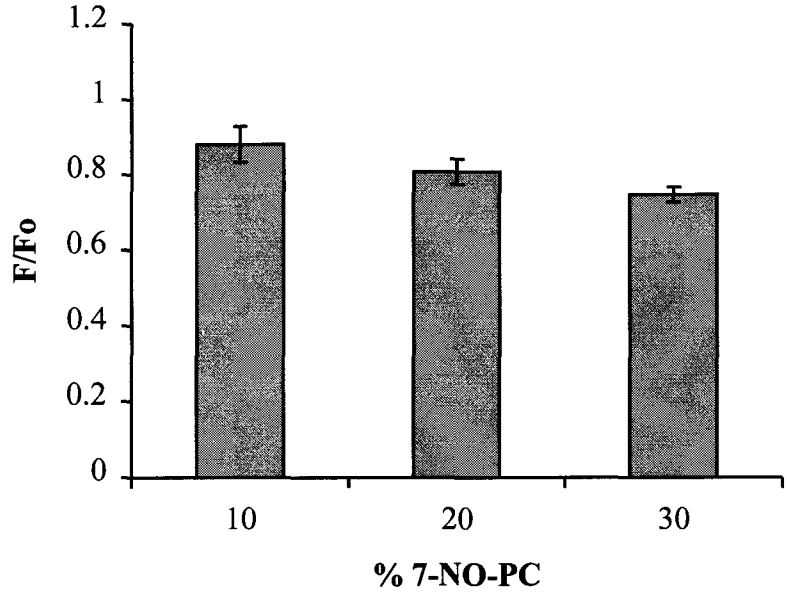

Figure 18: **Quenching of NBD-X_L by 7-NO-PC.**
Quenching was carried out as described in Section 2.6.3 and Section 3.4.3. Each column represents the mean value of F/Fo for three independent experiments, where F is the fluorescence intensity of NBD-X_L bound to liposomes containing the indicated amount of 7-NO-PC, and Fo is the intensity of NBD-X_L bound to liposomes lacking 7-NO-PC. The error bars represent the standard error of the mean (n=3).

Since not all of the NBD-X_L binds to the liposomes (see Figure 8) and no attempt was made to separate the two populations of NBD-X_L (bound and unbound), the degree of binding of NBD-X_L to the liposomes used in these quenching experiments was assessed. Following the fluorescence measurements the NBD-X_L/liposome mixtures were

subjected to a flotation assay. The amount of NBD-X_L in each fraction was quantified by western blot. Unlike the previously described quantitative western blots, these blots were fairly reproducible and the signal from the unknowns consistently fell within the linear range of the standards. The unknowns only had to be diluted in a 1:1 ratio with loading buffer, hopefully minimizing the effect of pipet error. Also the makeup of each of the samples compared was identical (only the percentage of 7-NO-PC in the liposomes changed) so any systematic errors would presumably be the same for all the samples and would therefore cancel out. Figure 19A shows an example of one of the quantitative western blots, and the data calculated from the blot is shown in Figures 19B and 19C. Figure 20 shows that the percentage of NBD-X_L which bound to the liposomes varied between 30 and 40%. Therefore, the decrease in fluorescence intensity seen in Figure 18 was probably not due to a similar decrease in the amount of NBD-X_L which bound to the liposomes. Furthermore, this result indicates that most of the NBD-X_L bound to the liposomes was quenched by the presence of 30% 7-NO-PC. In addition, the measured percentage of NBD-X_L which bound to the liposomes agrees reasonably well with the iodide ion quenching data discussed in Section 3.4.1 which indicated that approximately 38% of the NBD-X_L incubated with liposomes was protected from quenching by 0.1M iodide ions.

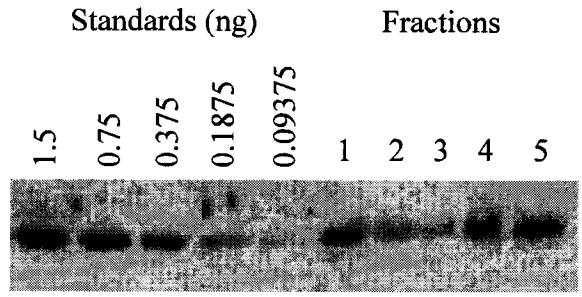

Figure 19A: Quantitative western blot of liposome-bound NBD-X_L.
A representative western blot used to quantify the amount of NBD-X_L in each fraction of the flotation assay. Known amounts of NBD-X_L were loaded in the first five lanes to act as standards (1.5, 0.75, 0.375, 0.1875, 0.09375 ng). The image was acquired as described in Section 2.7.

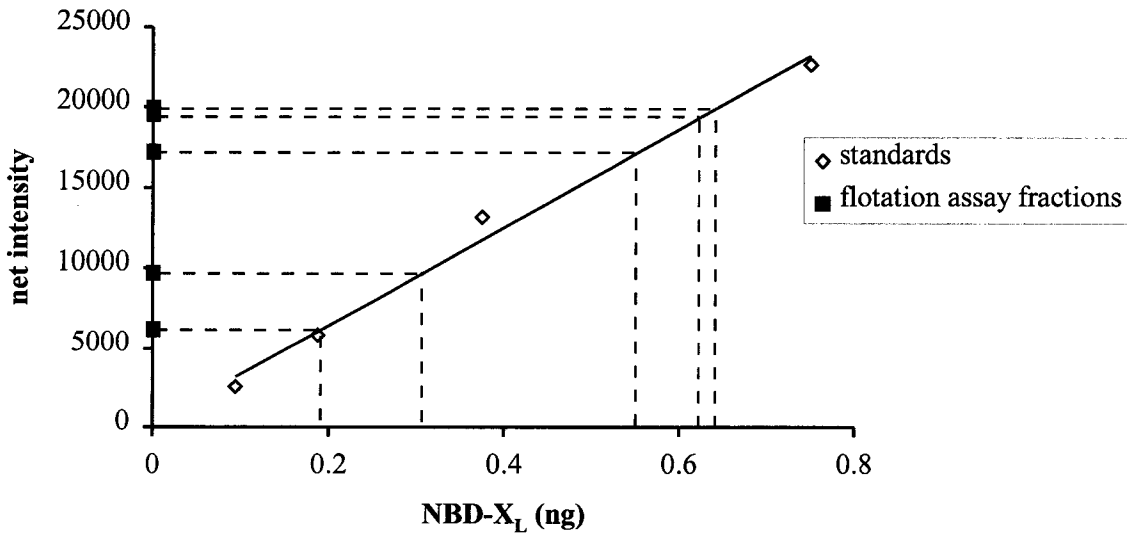

Figure 19B: Quantification of NBD-X_L by western blot.
A plot of net intensity of the chemiluminescence signal versus amount of NBD-X_L. The amount of NBD-X_L in each unknown lane in Figure 19A was calculated from the measured net intensity (values are shown on the graph) and the standard curve.

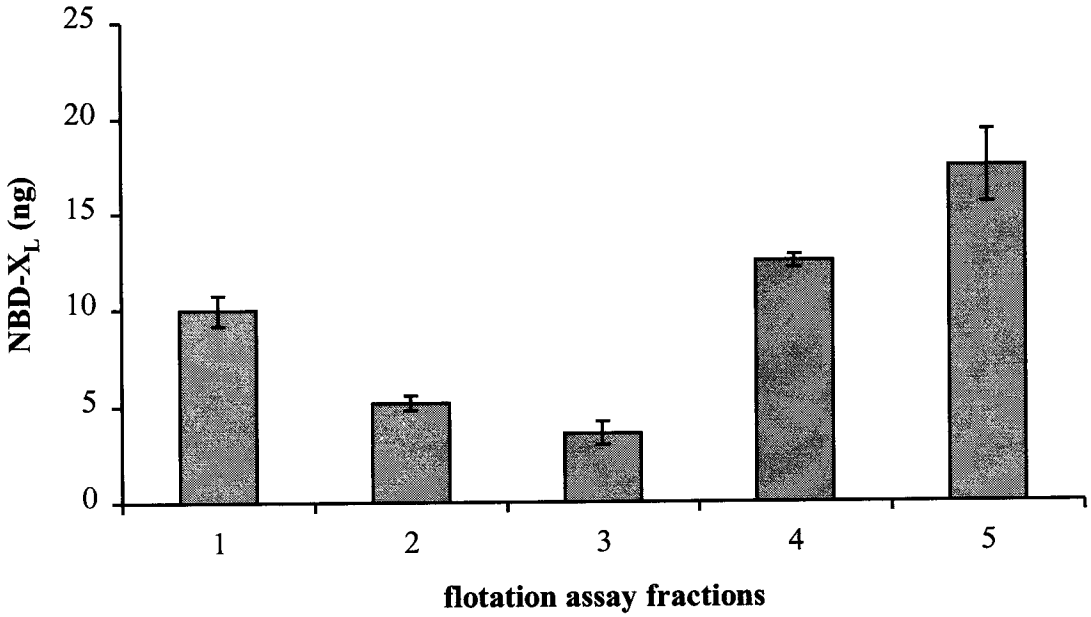

Figure 19C: Amount of NBD-X_L in each flotation assay fraction.
The total amount of NBD-X_L in each fraction of the flotation assay was calculated from the amounts of NBD-X_L measured in each lane of the western blot. The columns represent the mean amounts determined from four separate repetitions of the western blot seen in Figure 19A. The error bars represent the calculated standard error of the mean (n=4).

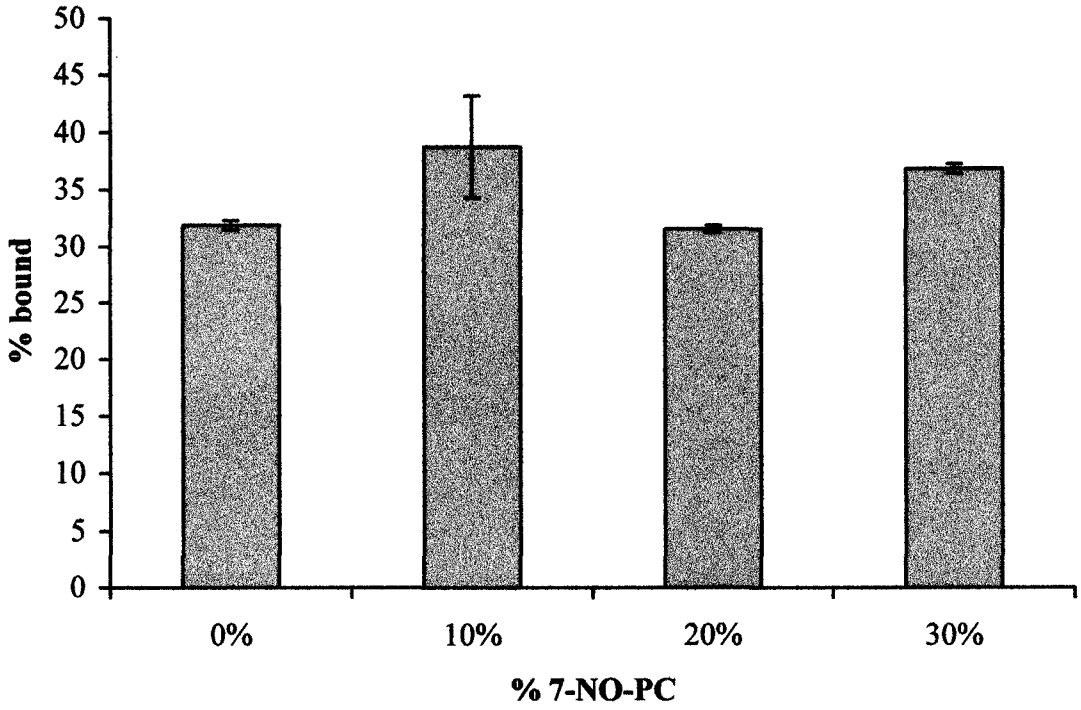

Figure 20: **Percentage of NBD-X_L bound to each type of LUV.**
The percentage of NBD-X_L bound to the liposomes used in the lipophilic quenching experiments was determined as described in the text and the captions to Figure 19. The amount of NBD-X_L in fractions 1 and 2 is considered the amount bound to LUVs and is expressed as a percentage of the total amount of NBD-X_L recovered from the flotation assay. Each column represents the mean percent bound from two separate experiments. The error bars represent the deviation from the mean.

Chapter 4: Discussion

The published structural data on Bcl-X_L (Muchmore *et al.*, 1996) prompted numerous subsequent pore-forming studies, as well as a great deal of speculation on the role of membrane-binding in the function of anti-apoptotic Bcl-2 family members. However there is virtually no published research regarding the membrane topology of Bcl-2 or Bcl-X_L. The one existing published study that attempted to address this topic used detergent micelles as a substitute for a membrane bilayer and a truncated Bcl-X_L molecule that lacked the C-terminal insertion sequence and a 40 amino acid region between BH4 and BH3 (Losonczi *et al.*, 2000).

Many of the studies using bacterially-expressed Bcl-X_L have used protein lacking the hydrophobic C-terminal sequence, which is necessary for targeting the protein to intracellular membranes. In addition, harsh denaturing methods are often needed to purify the protein. Use of the IMPACT™ system and very low concentrations of detergent allows for a much milder purification protocol, without the need to denature and then refold the protein, or to resolubilize it from the cell pellet following cell lysis.

The data presented in this thesis has shown that Bcl-X_L is capable of binding isolated ER microsomes *in vitro*. Although very little research has been directed towards a role for Bcl-X_L at the endoplasmic reticulum, it has been found to associate with some ER proteins (Ng and Shore, 1998). ER-localized Bcl-2 is capable of inhibiting apoptosis

initiated by certain stimuli (Zhu *et al.*, 1996; Annis *et al.*, 2001) and some preliminary data also indicates that a Bcl-X_L mutant that targets specifically to the ER is partially effective at inhibiting apoptosis (Aline Fiebig and David Andrews, McMaster University, personal communication). Apoptosis can be induced in some cell types by factors that cause the release of calcium from the ER, and both Bcl-2 and Bcl-X_L have been effective in inhibiting this apoptosis (He *et al.*, 1997; Pan *et al.*, 2000). However the mechanism of this inhibition is not clear, nor was the subcellular localization of Bcl-2 or Bcl-X_L determined in these studies.

The bulk of the published literature regarding Bcl-X_L has been devoted to its role at the mitochondrial outer membrane. I was not able to achieve significant binding of Bcl-X_L to isolated rat liver mitochondria. Mitochondria isolated by the method outlined in Section 2.4.2 have been successfully used in the past to study targeting of *in vitro* synthesized Bcl-2 (Janiak *et al.*, 1994a). The mitochondria used in this particular experiment (Figure 7) showed very poor pOCTgPA translocation, possibly indicating that the electrochemical gradient across the inner mitochondrial membrane was no longer intact in many of the mitochondria. Therefore the lack of Bcl-X_L association may be due to inferior mitochondrial preparations. Alternatively, it may simply require a larger amount of mitochondria to achieve significant binding of Bcl-X_L. In Figure 7, the amount of cytochrome b5 bound to mitochondria increases with increasing amounts of mitochondria present, indicating that even at the highest concentration of mitochondria used, maximum binding has not been reached. The amount of protein produced by *in vitro* translation is generally in the fmol range, and I was attempting to bind a

considerably larger amount of purified Bcl-X_L (1 μg = 38 pmol) to the mitochondria in this experiment. The published research involving Bcl-X_L and purified rat liver mitochondria usually reports the effect on cytochrome c release caused by incubating Bcl-X_L with the mitochondria. Virtually none of these studies give any indication of the amount of protein that actually associates with the mitochondria, making it difficult to compare my results with those of other researchers. In the sole study I have been able to find that measures binding of Bcl-X_L to rat liver mitochondria, 100 μg of mitochondrial protein were needed to achieve maximum binding of 1-2 fmol of *in vitro* synthesized Bcl-X_L (Tremblais *et al.*, 1999). This supports the possibility that a much higher amount of mitochondria would have been needed to see significant binding of the 1 μg of purified Bcl-X_L used in this experiment. In the future, once optimum binding of Bcl-X_L to mitochondria has been achieved, it will be interesting to compare the membrane topology of Bcl-X_L at the mitochondria with that of Bcl-X_L at the ER.

Three complementary fluorescence-based techniques were used to investigate whether a specific amino acid in the anti-apoptotic protein Bcl-X_L is inserted into the lipid bilayer upon binding of Bcl-X_L to either ER microsomes or liposomes. Environment-sensitive dyes such as NBD have been used to study the membrane topology of a number of different proteins. NBD is particularly useful since it is relatively small and therefore would not be expected to greatly perturb the native structure of the protein. Unlike some other environment-sensitive dyes, such as acrylodan, NBD is not hydrophobic enough to artifactually force insertion into the membrane (Shepard *et al.*, 1997).

The labelling efficiency of Bcl-X_L generally varies between 50% and 70%, whereas for the negative control Bcl-C151S it is between 45% and 55%. It is possible therefore that 45% to 55% of the dyes on Bcl-X_L are non-covalently associated with areas of the protein other than Cys151. However the fluorescent signal in the SDS-PAGE gel shown in Figure 12B is emitted only by the covalently-associated NBD molecules. The protein preparations used in this experiment gave labelling efficiencies of 58% (NBD-X_L) and 55% (NBD-C151S). Using the above assumption, this would indicate that only 3% of the protein seen in Figure 12 (upper panel) was responsible for the fluorescent signal in the lower panel of Figure 12. This seems unlikely given the strength of the fluorescent signal. A more plausible explanation for Figure 12 is that the NBD molecules capable of associating with Bcl-X_L bind to the available reactive group, and only in the absence of any reactive group do they remain non-covalently associated.

It would be preferable to eliminate the possibility of any non-specific binding of NBD to Bcl-X_L and this might be achieved in future by using different quenchers for the labelling reaction. I used DTT to react with any remaining NBD following the labelling reaction. A more polar or charged reactive molecule, such as cysteine which has two charges, might prevent any hydrophobic interactions occurring between the protein and the free NBD. Alternatively, decreasing the amount of NBD in the labelling reaction might decrease the amount of non-specific association, although likely at the expense of the efficiency of the covalent reaction with Cys151.

The environmental sensitivity of NBD manifests as characteristic changes in the emission properties of the molecule. Increasing the hydrophobicity of the environment

surrounding the dye generally results in a large increase in emission intensity, and a decrease in the maximum emission wavelength. Therefore a straight-forward and relatively simple initial experiment is to compare the emission properties of NBD-labelled Bcl-X_L before and after binding to membranes. Upon binding of Bcl-X_L to ER microsomes (EKRMs) there is only a slight increase in emission intensity (Figure 14), and the maximum emission wavelength also does not change significantly (data not shown). Taken at face value this would suggest that Cys151 is not inserted into the membrane following binding, however it is not possible to interpret the results of this one technique quite so unambiguously. Even in the soluble, non-membrane-bound protein, the maximum emission wavelength of the NBD molecules (~525-530 nm) suggests that Cys151 is already in a hydrophobic environment. This result is supported by the crystal structure of Bcl-X_L (Muchmore *et al.*, 1996) which shows that the side chain of Cys151 extends out from helix α5 towards the hydrophobic face of helix α1, and into a pocket formed by two Leucine residues. Therefore an alternate interpretation of Figure 14 is that the small change in fluorescence intensity upon membrane binding is due to movement from a nonpolar area within the protein to another only slightly more nonpolar environment (the membrane).

A third explanation for Figure 14 is the existence of multiple forms of Bcl-X_L, only some of which have Cys151 inserted into the bilayer. Steady-state fluorescence emission readings average the fluorescent signal from all of the NBD molecules present and will mask any sample heterogeneity. There are at least two forms of Bcl-X_L present in the sample measured in Figure 14, membrane-bound and non-membrane-bound. Even

within the membrane-bound population there may be more than one conformation of Bcl-X_L, for example some of the molecules may have several of their helices integrated into the membrane whereas in others the bulk of the protein is soluble and only the C-terminal insertion sequence is bound to the membrane. Time-resolved lifetime measurements would be necessary to rigorously determine sample heterogeneity. NBD fluorescence lifetimes are sensitive to hydrophobicity, a dye in an aqueous environment has a short lifetime (~1 ns) while in a nonpolar environment the lifetime increases significantly (7-8 ns). In addition, different populations having different lifetimes can be distinguished, as well as the percentage of molecules in each population.

In contrast to the data obtained with EKRMs, binding of NBD-X_L to liposomes (60% DOPC, 40% DOPG) caused a significant increase in emission intensity (Figure 16), despite the fact that only approximately one third of the protein was actually bound to the liposomes (Figure 20). This difference in behaviour between the two types of bilayer may be due to the fact that NBD-X_L does not assume the same structure in EKRMs as in liposomes (i.e. Cys151 may insert into the bilayer in liposomes more efficiently than into microsomes). Alternatively the environment within the microsome bilayer where Cys151 is located may not be as hydrophobic as the interior of a pure lipid bilayer, or there may be quenchers naturally present within the microsome bilayer which decrease the fluorescent intensity.

An alternate fluorescent technique for studying membrane topology is to measure the accessibility of a fluorescently-labelled amino acid to both soluble and lipophilic quenchers. The Ksv values for soluble and liposome-bound NBD-X_L, as well as the 7-

NO-PC quenching data, indicate that virtually all of the NBD-X_L that binds to the liposomes has Cys151 inserted into the bilayer. This is consistent with the emission intensity increase seen in Figure 16. In addition, the Ksv value for EKRM-bound NBD-X_L indicates that Cys151 is also protected from aqueous quenchers in this system, despite the apparent lack of a significant emission intensity increase. This strongly suggests that at least some proportion of EKRM-bound Bcl-X_L has inserted Cys151 into the bilayer.

While my data indicates that Cys151 is inserted into the bilayer, it cannot be ascertained how deeply into the membrane the tip of the α5 helix penetrates. Future experiments using quenchers located at different positions along the acyl chain can be used to more rigorously map the location of Cys151 within the bilayer. As well, a series of Bcl-X_L mutants with single cysteines placed along the length of the α5 and α6 helices can be used to determine the membrane topology of this entire region.

To summarize, when NBD-labelled Bcl-X_L is incubated with liposomes, the emission intensity of the dye increases significantly, and the fraction of the NBD molecules protected from quenching by aqueous iodide ions is consistent with the fraction of Bcl-X_L that binds to the liposomes. A similar fraction of the fluorescence intensity can be quenched by quenchers restricted to the interior of the bilayer. These results strongly suggest that liposome-bound Bcl-X_L has inserted Cys151 into the bilayer. Microsome-bound NBD-labelled Bcl-X_L is also significantly protected from iodide quenching, suggesting insertion of Cys151 into the bilayer, although it does not display the characteristic emission intensity increase. This may be due to a difference in the internal environment of the membrane bilayer between liposomes and microsomes.

The data presented in this thesis suggests that Cys151, located near the C-terminal end of the α5 helix, is inserted into the lipid bilayer when full-length Bcl-X_L is bound to membranes. The similarity in structure of Bcl-X_L to some bacterial pore-forming toxins suggested that Bcl-2 family members could form pores by inserting their α5 and α6 helices perpendicularly across the membrane bilayer. However the results of actual pore-forming studies on anti-apoptotic proteins remain ambiguous. Acidic pH was required for induction of bulk ion efflux from lipid vesicles by Bcl-2 and Bcl-X_L, suggesting that only at low pH could a significant fraction of the protein molecules present form pores (Minn *et al.*, 1997; Schendel *et al.*, 1997). However the proteins used in most of these studies had deletions at the C termini, removing the membrane anchoring region. Without this region, Bcl-2 and Bcl-X_L can bind to lipid vesicles only at acidic pH, not neutral pH (Schendel *et al.*, 1997; Basañez *et al.*, 2001). Single channel conductances have been measured for full-length Bcl-X_L at neutral pH (Lam *et al.*, 1998) however it is not clear if these channels represent a common behaviour of Bcl-X_L molecules or were formed by a rare sub-population of molecules. At neutral pH Bax and pro-apoptotic cleavage products of Bcl-X_L can release encapsulated fluorescent dyes from lipid vesicles (Antonsson *et al.*, 1997; Basañez *et al.*, 2001) but full-length Bcl-X_L cannot, even though it binds to the vesicles to a similar extent (Basañez *et al.*, 2001). Taken together, current evidence favours a model where pro-apoptotic proteins do form pores, either alone or in conjunction with other membrane proteins, disrupting ion gradients or releasing apoptogenic factors such as cytochrome c from mitochondria. However, it is unclear whether anti-apoptotic proteins also form pores.

Other models for Bcl-2/Bcl-X_L function include inhibition of the channels formed by pro-apoptotic proteins, sequestering pro-apoptotic factors on membrane surfaces (the *C. elegans* model), or regulation of mitochondrial membrane permeability by affecting the function of the voltage-dependent anion channel (VDAC). None of these functions are strictly incompatible with a Bcl-X_L structure that has at least part of the α5 helix inserted into the membrane. Bcl-X_L is believed to regulate VDAC through its BH4 domain, although the exact nature of its effect on this channel has been disputed (Shimizu *et al.*, 2000; Vander Heiden *et al.*, 2001). The conformational change in Bcl-X_L required for membrane insertion of α5/α6 may free the BH4 domain to interact with VDAC, or with one or more of the other apoptosis-related proteins that it has been suggested to associate with (reviewed in Schendel *et al.*, 1998).

In conclusion, the data presented in this thesis indicates that when the anti-apoptotic protein Bcl-X_L binds to membranes *in vitro* it adopts a conformation whereby Cys151, located near the C-terminal end of the α5 helix, inserts into the membrane bilayer. Furthermore these results suggest that fluorescence-based techniques are viable methods for studying the membrane topology of Bcl-X_L *in vitro*. The methods presented in this thesis will be useful in determining the complete membrane topology of Bcl-X_L localized to both ER and mitochondria, as well as potentially characterizing changes in the structure caused by the addition of apoptotic factors such as pro-apoptotic family members or cytosol isolated from cells undergoing apoptosis.

Chapter 5: References

Adams, J. M., and Cory, S. (1998). The Bcl-2 Protein Family: Arbiters of Cell Survival. *Science*. 281: 1322-1326.

Annis, M. G., Zamzami, N., Zhu, W., Penn, L. Z., Kroemer, G., Leber, B., and Andrews, D. W. (2001). Endoplasmic reticulum localized Bcl-2 prevents apoptosis when redistribution of cytochrome *c* is a late event. *Oncogene*. 20: 1939-1952.

Antonsson, B., Conti, F., Ciavatta, A., Montessuit, S., Lewis, S., Martinou, I., Bernasconi, L., Bernard, A., Mermod, J.-J., Mazzei, G., Maundrell, K., Gambale, F., Sadoul, R., and Martinou, J.-C. (1997). Inhibition of Bax Channel-Forming Activity by Bcl-2. *Science*. 277: 370-372.

Basañez, G., Zhang, J., Chau, B. N., Maksaev, G. I., Frolov, V. A., Brandt, T. A., Burch, J., Hardwick, J. M., and Zimmerberg, J. (2001). Pro-apoptotic Cleavage Products of Bcl-X_L Form Cytochrome c-conducting Pores in Pure Lipid Membranes. *J. Biol. Chem*. 276: 31083-31091.

Bennett, M. J., Choe, S., and Eisenberg, D. (1994). Domain swapping: Entangling alliances between proteins. *Proc. Natl. Acad. Sci. USA*. 91: 3127-3131.

Boise, L. H., González-Garcia, M., Postema, C. E., Ding, L., Lindsten, T., Turka, L. A., Mao, X., Nuñez, G., and Thompson, C. B. (1993). *bcl-x*, a *bcl-2*-Related Gene that Functions as a Dominant Regulator of Apoptotic Cell Death. *Cell*. 74: 597-608.

Chinnaiyan, A. M., O'Rourke, K., Lane, B. R., and Dixit, V. M. (1997). Interaction of CED-4 with CED-3 and CED-9: a molecular framework for cell death. *Science*. 275: 1122-1126.

Choe, S., Bennett, M. J., Fujii, G., Curmi, P. M. G., Kantardjieff, K. A., Collier, R. J., and Eisenberg, D. (1992). The crystal structure of diphtheria toxin. *Nature*. 357: 216-222.

Cleary, M. L., Smith, S. D., and Sklar, J. (1986). Cloning and Structural Analysis of cDNAs for bcl-2 and a Hybrid bcl-2/Immunoglobulin Transcript Resulting from the t(14;18) Translocation. *Cell.* 47: 19-28.

Conradt, B. and Horvitz, H. R. (1998). The *C. elegans* Protein EGL-1 is Required for Programmed Cell Death and Interacts with the Bcl-2-like Protein CED-9. *Cell.* 93: 519-529.

Ellis, H. M., and Horvitz, H. R. (1986). Genetic control of programmed cell death in the nematode *C. elegans*. *Cell.* 44: 817-829.

Falcone, D.,and Andrews, D. W. (1991). Both the 5' Untranslated Region and the Sequences Surrounding the Start Site Contribute to Efficient Initiation of Translation In Vitro. *Mol. Cell. Biol.* 11: 2656-2664.

Gill, S. C., and von Hippel, P. H. (1989). Calculation of Protein Extinction Coefficients from Amino Acid Sequence Data. *Anal. Biochem.* 182: 319-326.

González-Garcia, M., Pérez-Ballestero, R., Ding, L., Duan, L., Boise, L. H., Thompson, C. B., and Nuñez, G. (1994). Bcl-X_L is the major bcl-x mRNA form expressed during murine development and its product localizes to mitochondria. *Development.* 120: 3033-3042.

Greenawalt, J. W. (1974). The Isolation of Outer and Inner Mitochondrial Membranes. *Meth. Enzym.* 31: 310-323.

Gross, A., McDonnell, J. M., and Korsmeyer, S. J. (1999). BCL-2 family members and the mitochondria in apoptosis. *Genes Dev.* 13: 1899-1911.

Gurevich, V. V., Pokrovskaya, I. D., Obukhova, T. A., and Zozulya, S. A. (1991). Preparative *in Vitro* mRNA Synthesis Using Sp6 and T7 RNA Polymerases. *Anal. Biochem.* 195: 207-213.

He, H., Lam, M., McCormick, T. S., and Distelhorst, C. W. (1997). Maintenance of calcium homeostasis in Endoplasmic Reticulum by Bcl-2. *J. Cell. Biol.* 138: 1219-1228.

Hengartner, M. O., Ellis, R. E., and Horvitz, H. R. (1992). *C. elegans* gene ced-9 protects cells from programmed cell death. *Nature.* 356: 494-499.

Horvitz, H. R. (1999). Genetic Control of Programmed Cell Death in the Nematode *Caenorhabditis elegans*. *Cancer Research (Suppl.).* 59: 1701s-1706s.

Hsu, Y.-T., Wolter, K. G., and Youle, R. J. (1997) Cytosol-to-membrane redistribution of Bax and Bcl-X_L during apoptosis. *Proc. Natl. Acad. Sci. USA*. 94: 3668-3672.

Hsu, Y.-T., and Youle, R. J. (1997). Nonionic Detergents Induce Dimerization among Members of the Bcl-2 Family. *J. Biol. Chem.* 272: 13829-13834.

Hughes, M. J. G., and Andrews, D. W. (1996). Creation of Deletion, Insertion and Substitution Mutations Using a Single Pair of Primers and PCR. *BioTechniques*. 20: 188-196.

Jackson, R. J., and Hunt, T. (1983). Preparation and Use of Nuclease-Treated Rabbit Reticulocyte Lysates for the Translation of Eukaryotic Messenger RNA. *Meth. Enzym.* 96: 50-74.

Janiak, F., Leber, B., and Andrews, D. W. (1994a). Assembly of Bcl-2 into Microsomal and Outer Mitochondrial Membranes. *J. Biol. Chem.* 269: 9842-9849.

Janiak, F., Glover, J. R., Leber, B., Rachubinski, R. A., and Andrews, D. W. (1994b). Targeting of passenger protein domains to multiple intracellular membranes. *Biochem J.* 300: 191-199.

Jiang, J. X., Chung, L. A., and London, E. (1991). Self-translocation of Diphtheria Toxin across Model Membranes. *J. Biol. Chem.* 266: 24003-24010.

Kim, P. K., Janiak-Spens, F., Trimble, W. S., Leber, B., and Andrews, D. W. (1997). Evidence for multiple mechanisms for membrane binding and integration via carboxyl-terminal insertion sequences. *Biochemistry*. 36: 8873-8882.

Korsmeyer, S. J. (1999). BCL-2 Gene Family and the Regulation of Programmed Cell Death. *Cancer Research (Suppl.)*. 59: 1693s-1700s.

Lakowicz, J. R. (1999). *Principles of Fluorescence Spectroscopy, 2nd ed.* Kluwer Academic/Plenum Publishers. New York.

Lam, M., Bhat, M. B., Nuñez, G., Ma, J., and Distelhorst, C. W. (1998). Regulation of Bcl-xl Channel Activity by Calcium. *J. Biol. Chem.* 273: 17307-17310.

Losonczi, J. A., Olejniczak, E. T., Betz, S. F., Harlan, J. E., Mack, J. and Fesik, S. W. (2000). NMR Studies of the Anti-Apoptotic Protein Bcl-X_L in Micelles. *Biochemistry*. 39: 11024-11033.

Minn, A. J., Vélez, P., Schendel, S. L., Liang, H., Muchmore, S. W., Fesik, S. W., Fill, M., and Thompson, C. B. (1997). Bcl-X_L forms an ion channel in synthetic lipid membranes. *Nature*. 385: 353-357.

Motoyama, N., Wang, F., Roth, K. A., Sawa, H., Nakayama, K.-i., Nakayama, K., Negishi, I., Senju, S., Zhang, Q., Fujii, S., and Loh, D. Y. (1995). Massive Cell Death of Immature Hematopoietic Cells and Neurons in Bcl-X-Deficient Mice. *Science*. 267: 1506-1510.

Muchmore, S. W., Sattler, M., Liang, H., Meadows, R. P., Harlan, J. E., Yoon, H. S., Nettesheim, D., Chang, B. S., Thompson, C. B., Wong, S.-L., Ng, S.-C., and Fesik, S. W. (1996). X-ray and NMR structure of human Bcl-XL, an inhibitor of programmed cell death. *Nature*. 381: 335-341.

Ng, F., and Shore, G. C. (1998). Bcl-X_L Cooperatively Associates with the Bap31 Complex in the Endoplasmic Reticulum, Dependent on Procaspase-8 and Ced-4 Adaptor. *J. Biol. Chem.* 273: 3140-3143.

Nguyen, M., Branton, P. E., Walton, P. A., Oltvai, Z. N., Korsmeyer, S. J., and Shore, G. C. (1994). Role of membrane anchor domain of Bcl-2 in suppression of apoptosis caused by E1B-defective adenovirus. *J. Biol. Chem.* 268: 25265-25268.

Pan, G., O'Rourke, K., and Dixit, V. M. (1998). Caspase-9, Bcl-X_L, and Apaf-1 Form a Ternary Complex. *J. Biol. Chem.* 273: 5841-5845.

Pan, Z., Damron, D., Nieminen, A.-L., Bhat, M. B., and Ma, J. (2000). Depletion of intracellular Ca^{2+} by caffeine and ryanodine induces apoptosis of chinese hamster ovary cells transfected with ryanodine receptor. *J. Biol. Chem.* 275: 19978-19984.

Rao, L., and White, E. (1997). Bcl-2 and the ICE family of apoptotic regulators: making a connection. *Curr. Opin. Genet. Dev.* 7: 52-58.

Reed, J. C. (1997). Double identity for proteins of the Bcl-2 family. *Nature*. 387: 773-776.

Ren, J., Sharpe, J. C., Collier, R. J., and London, E. (1999) Membrane Translocation of Charged Residues at the Tips of Hydrophobic Helices in the T Domain of Diphtheria Toxin. *Biochemistry*. 38: 976-984.

Sattler, M., Liang, H., Nettesheim, D., Meadows, R. P., Harlan, J. E., Eberstadt, M., Yoon, H. S., Shuker, S. B., Chang, B. S., Minn, A. J., Thompson, C. B., and Fesik, S. W. (1997). Structure of Bcl-X_L Peptide Complex: Recognition Between Regulators of Apoptosis. *Science*. 275: 983-986.

Schendel, S. L., Xie, Z., Oblatt Montal, M., Matsuyama, S., Montal, M., and Reed, J. C. (1997). Channel formation by antiapoptotic protein Bcl-2. *Proc. Natl. Acad. Sci. USA*. 94: 5113-5118.

Schendel, S. L., Montal, M., Reed, J. C. (1998). Bcl-2 family proteins as ion-channels. *Cell Death Diff.* 5: 372-380.

Schlesinger, P. H., Gross, A., Yin, X.-M., Yamamoto, K., Saito, M., Waksman, G., and Korsmeyer, S. J. (1997) Comparison of the ion channel characteristics of proapoptotic Bax and antiapoptotic Bcl-2. *Proc. Natl. Acad. Sci. USA*. 94: 11357-11362.

Shagger, H., and von Jagow, G. (1987). Tricine-Sodium Dodecyl Sulfate-Polyacrylamide Gel Electrophoresis for the Separation of Proteins in the Range from 1 to 100 kDa. *Anal. Biochem.* 166: 368-379.

Shepard, L. A., Heuck, A. P., Hamman, B. D., Rossjohn, J., Parker, M. W., Ryan, K. R., Johnson, A. E., Tweten, R. K. (1998). Identification of a membrane-spanning domain of the thiol-activated pore-forming toxin *Clostridium perfringens* Perfringolysin O: An α-helical to β-sheet transition identified by fluorescence spectroscopy. *Biochemistry*. 37: 14563-14574.

Shimizu, S., Konishi, A., Kodama, T., and Tsujimoto, Y. (2000). BH4 domain of antiapoptotic Bcl-2 family members closes voltage-dependent anion channel and inhibits apoptotic mitochondrial changes and cell death. *Proc. Natl. Acad. Sci. USA*. 97: 3100-3105.

Thompson, C. B. (1995). Apoptosis in the pathogenesis and treatment of disease. *Science*. 267: 1456-1462.

Thornberry, N. A., and Lazebnik, Y. (1998). Caspases: Enemies Within. *Science*. 281: 1312-1316.

Tremblais, K., Oliver, L., Juin, P., Le Cabellec, M. T., Meflah, K., and Vallette, F. M. (1999). The C-terminus of bax is not a Membrane Addressing/Anchoring Signal. *Biochem Biophys Res Commun*. 260: 582-591.

Vander Heiden, M. G., Li, X. X., Gottleib, E., Hill, R. B., Thompson, C. B., and Colombini, M. (2001). Bcl-X_L Promotes the Open Configuration of VDAC and Metabolite Passage through the Outer Mitochondrial Membrane. *J. Biol. Chem.* 276: 19414-19419.

Walter, P., and Blobel, G. (1983). Preparation of Microsomal Membranes for Cotranslational Protein Translocation. *Meth. Enzym.* 96: 84-93.

White, E. (1996). Life, death, and the pursuit of apoptosis. *Genes Dev.* 10: 1-15.

Wolter, K. G., Hsu, Y.-T., Smith, C. L., Nechushtan, A., Xi, X.-G., and Youle, R. J. (1997). Movement of Bax from the Cytosol to Mitochondria during Apoptosis. *J. Cell. Biol.* 139: 1281-1292.

Wyllie, A. H., Kerr, J. F. R., and Currie, A. R. (1980). Cell death: The significance of apoptosis. *Int. Rev. Cytol.* 68: 251-306.

Yin, X.-M., Oltvai, Z., and Korsmeyer, S. (1994). BH1 and BH2 domains of Bcl-2 are required for inhibition of apoptosis and heterodimerization with Bax. *Nature.* 369: 321-323.

Young, J. C., Ursini, J., Legate, K. R., Miller, J. D., Walter, P., and Andrews, D. W. (1995). An Amino-terminal Domain containing Hydrophobic and Hydrophilic Sequences Binds the Signal Recognition Particle Receptor α Subunit to the β Subunit on the Endoplasmic Reticulum Membrane. *J. Biol. Chem.* 270: 15650-15657.

Zha, H., Aime-Sempe, C., Sato, T., and Reed, J. C. (1996). Proapoptotic Protein Bax Heterodimerizes with Bcl-2 and Homodimerizes with Bax via a Novel Domain (BH3) Distinct from BH1 and BH2. *J. Biol. Chem.* 271: 7440-7444.

Zhu, W., Cowie, A., Wasfy, G. W., Penn, L. Z., Leber, B., and Andrews, D. W. (1996). Bcl-2 mutants with restricted subcellular location reveal spatially distinct pathways for apoptosis in different cell types. *EMBO J.* 15: 4130-4140.

Zou, H., Henzel, W. J., Liu, X., Lutschg, A., and Wang, X. (1997). Apaf-1, a Human Protein Homologous to *C. elegans* CED-4, Participates in Cytochrome c-dependent activation of Caspase-3. *Cell.* 90: 405-413.